Available online at www.sciencedirect.com
ScienceDirect
Bioorganic & Medicinal Chemistry Letters
ELSEVIER
Bioorganic & Medicinal Chemistry Letters xxx (2008) xxx–xxx

Sugar Chips immobilized with synthetic sulfated disaccharides of heparin/heparan sulfate partial structure☆

Masahiro Wakao,[a] Akihiro Saito,[a] Koh Ohishi,[a] Yuko Kishimoto,[b] Tomoaki Nishimura,[a,b] Michael Sobel[c] and Yasuo Suda[a,b,*]

[a]*Department of Nanostructure and Advanced Materials, Graduate School of Science and Engineering, Kagoshima University, 1-21-40 Korimoto, Kagoshima 890-0065, Japan*
[b]*SUDx-Biotec corporation, 5-5-2 Minatojima-cho, Kobe 650-0047, Japan*
[c]*Department of Surgery, University of Washington and VA Puget Sound Health Care System, Seattle, WA 98108, USA*

Received 21 August 2007; revised 24 December 2007; accepted 16 January 2008

Abstract—Carbohydrate chip technology has a great potential for the high-throughput evaluation of carbohydrate–protein interactions. Herein, we report syntheses of novel sulfated oligosaccharides possessing heparin and heparan sulfate partial disaccharide structures, their immobilization on gold-coated chips to prepare array-type Sugar Chips, and evaluation of binding potencies of proteins by surface plasmon resonance (SPR) imaging technology. Sulfated oligosaccharides were efficiently synthesized from glucosamine and uronic acid moieties. Synthesized sulfated oligosaccharides were then easily immobilized on gold-coated chips using previously reported methods. The effectiveness of this analytical method was confirmed in binding experiments between the chips and heparin binding proteins, fibronectin and recombinant human von Willebrand factor A1 domain (rh-vWf-A1), where specific partial structures of heparin or heparan sulfate responsible for binding were identified.

Carbohydrate chips and related array technologies[1–3] have attracted a great deal of attention as a powerful tool for glycomics. Like DNA[4] and protein chips,[5] they can rapidly and simply evaluate carbohydrate–protein interactions in parallel, with a minimum amount of sample. Our ongoing research involves this functional analysis of sulfated polysaccharides such as heparin (HP) and heparan sulfate (HS).[3a] HP and HS are highly sulfated polysaccharides and belong to the glycosaminoglycan (GAG) superfamily. They are among the most complex of carbohydrates, and play a significant role in biological processes through their binding interactions with numerous proteins,[6] such as growth factors, cytokines, viral proteins, and coagulation factors, among others. HP/HS have a basic structure composed of a repeating α or β(1,4)-linked disaccharide moiety which is derived from uronic acid (either glucuronic acid or iduronic acid) and *N*-acetyl-glucosamine residues. In general, HP/HS chains are very heterogeneous and contain innumerable substitution patterns due in part to some randomness in the multiple enzymatic modifications in their biosynthesis. This heterogeneity makes it difficult to elucidate the structure-function relationships of HP/HS at the molecular level. Therefore, structurally defined HP/HS sequences are necessary for the precise elucidation of the mode of HP/HS actions on their target molecules. So far, many synthetic efforts have been dedicated to the synthesis of HP/HS fragments.[3b–d,7,8]

Previously, we have reported that a specific disaccharide unit in HP, *O*-(2-deoxy-2-sulfamido-6-*O*-sulfo-α-D-glucopyranosyl)-(1-4)-2-*O*-sulfo-α-L-idopyranosyluronic acid (abbreviated as GlcNS6S-IdoA2S), is a key unit for binding to human platelets[9] and von Willebrand factor (vWf),[10] and that the clustering of these disaccharides significantly enhanced the interaction.[11,12] To systematically investigate heparin's binding properties, we have developed a method[3a] for the immobilization the sulfated oligosaccharide onto a gold-coated chip,

Keywords: Sugar; Carbohydrate; Chip; Heparin; Heparan sulfate; Carbohydrate–protein interaction; Surface plasmon resonance; SPR; SPR-imaging.
☆ Syntheses of sulfated oligosaccharide of heparin and heparan sulfate partial structures and their application to Sugar Chips are described.
* Corresponding author. Tel./fax: +81 99 285 8369; e-mail: ysuda@eng.kagoshima-u.ac.jp

0960-894X/$ - see front matter © 2008 Published by Elsevier Ltd.
doi:10.1016/j.bmcl.2008.01.069

and have devised an analytical system using surface plasmon resonance (SPR) technology, which permits their real-time study without further labeling. These systems can be applied to the investigation of the binding interactions of a variety of structurally defined oligosaccharides.

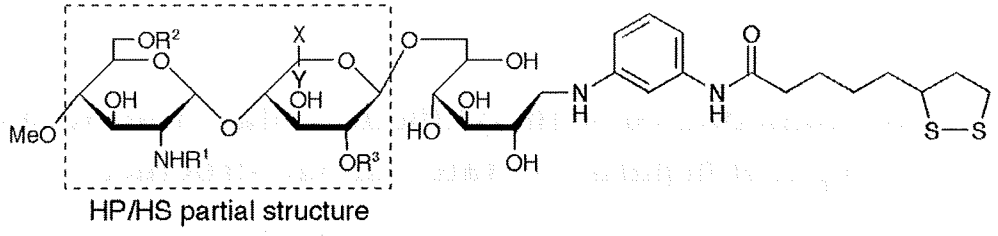

1, GlcNS6S-IdoA2S: $R^1=SO_3^-$, $R^2=SO_3^-$, $R^3=SO_3^-$, X=H, $Y=CO_2^-$
2, GlcNS-IdoA2S: $R^1=SO_3^-$, R^2=H, $R^3=SO_3^-$, X=H, $Y=CO_2^-$
3, GlcNS6S-GlcA: $R^1=SO_3^-$, $R^2=SO_3^-$, R^3=H, $X=CO_2^-$, Y=H
4, GlcNS-GlcA: $R^1=SO_3^-$, R^2=H, R^3=H, $X=CO_2^-$, Y=H

Figure 1. Sulfated disaccharide partial structures of heparin/heparan sulfate.

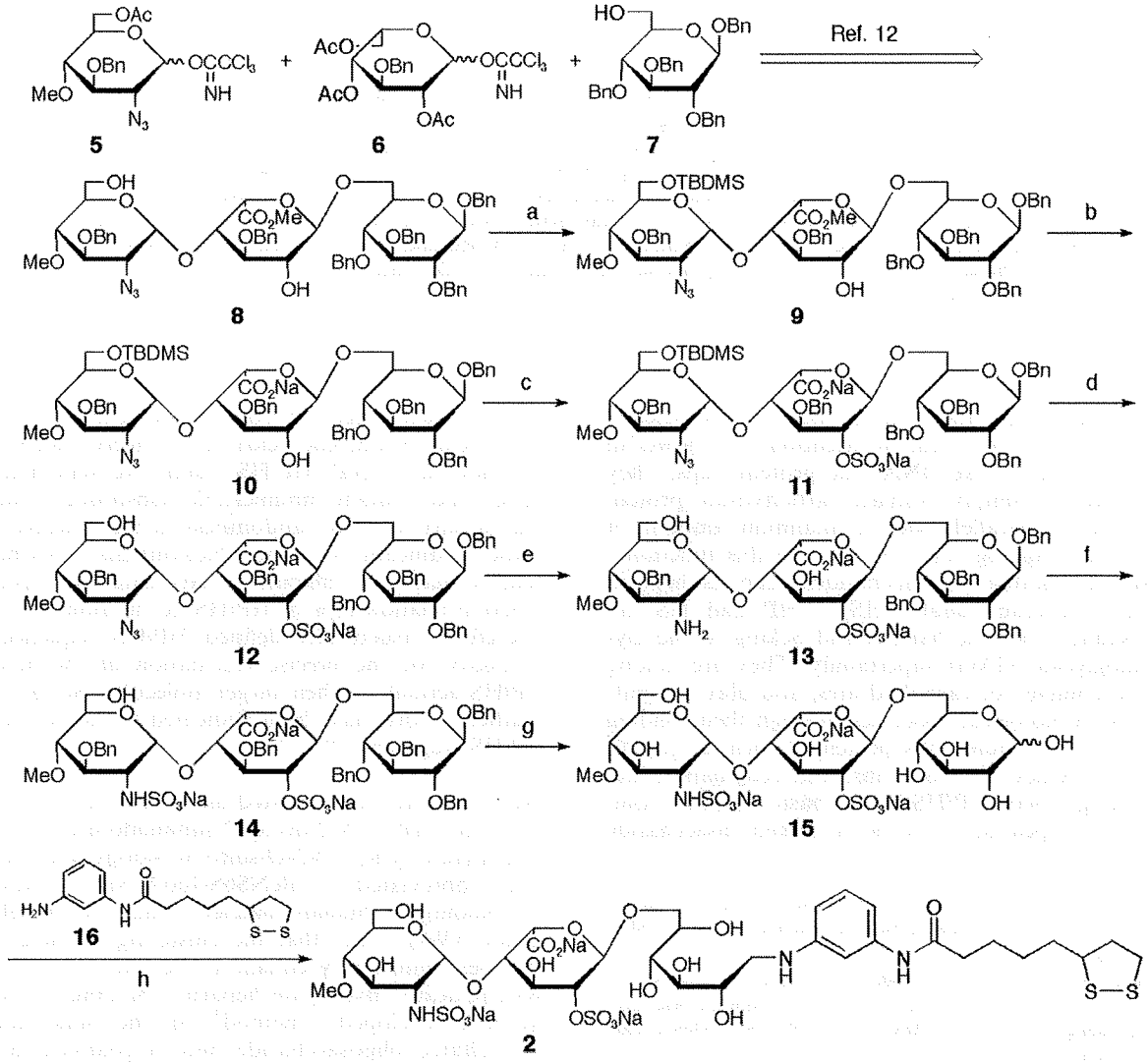

Scheme 1. Synthesis of ligand conjugate **2** containing GlcNS-IdoA2S. Reagents: (a) TBDMSCl, imidazole, MS4AP in CH_2Cl_2, 45%; (b) 1 M NaOH, MeOH/THF (1:1), 70%; (c) SO_3Pyr in Pyr; (d) HFPyr in Pyr; (e) 10% Pd–C, H_2 (1 kg/cm^2) in THF/MeOH (2:1); (f) SO_3Pyr in H_2O; (g) 10% Pd–C, H_2 (7 kg/cm^2) in H_2O/AcOH (5:1), 29% (5 steps); (h) $NaBH_3CN$ in DMAc/H_2O/AcOH (1:1:0.1), 82%.

Please cite this article in press as: Wakao, M. et al., *Bioorg. Med. Chem. Lett.* (2008), doi:10.1016/j.bmcl.2008.01.069

To better understand the HP/HS disaccharide structures involved in specific protein interactions, we designed three kinds of sulfated trisaccharide ligand conjugates **2**–**4** containing the disaccharide units as shown in Figure 1; GlcNS-IdoA2S (**2**): *O*-(2-deoxy-2-sulfamido-α-D-glucopyranosyl)-(1-4)-2-*O*-sulfo-α-L-idopyranosyluronic acid, GlcNS6S-GlcA (**3**): *O*-(2-deoxy-2-sulfamido-6-*O*-sulfo-α-D-glucopyranosyl)-(1-4)-α-D-glucopyranosyluronic acid, GlcNS-GlcA (**4**): *O*-(2-deoxy-2-sulfamido-α-D-glucopyranosyl)-(1-4)-α-D-glucopranosyluronic acid. The disaccharide units contained in ligand conjugates **1**–**4** of Figure 1 are frequently found in HP/HS disaccharide unit.

For efficient synthesis, four monomeric building blocks were prepared. 2-Azido glucose derivative **5**, idose derivative **6**, and 4,6-benzylidene glucose derivative **17** were used for glucosamine, iduronic acid, and glucuronic acid moieties, respectively. Selective sulfation onto glucosamine and iduronic acid or glucuronic acid moieties can be carried out by an appropriate functionalization. The 6-OH glucose derivative **7** was used as the reducing end for the conjugation to linker molecule **16** after deprotection on the glucose, which works not only as a reducing end donor for reductive amination but also as the hydrophilic moiety in the molecule to minimize any non-specific hydrophobic interactions between the linker and target proteins or cells.

The synthesis of ligand conjugate **2** containing GlcNS-IdoA2S unit was carried out as shown in Scheme 1. Trisaccharide **8**, which was prepared according to the method reported previously,[12] was selectively protected by *t*-butyldimethylsilyl (TBDMS) group. The methyl ester of trisaccharide **9** was hydrolyzed and the remaining 2′-hy-

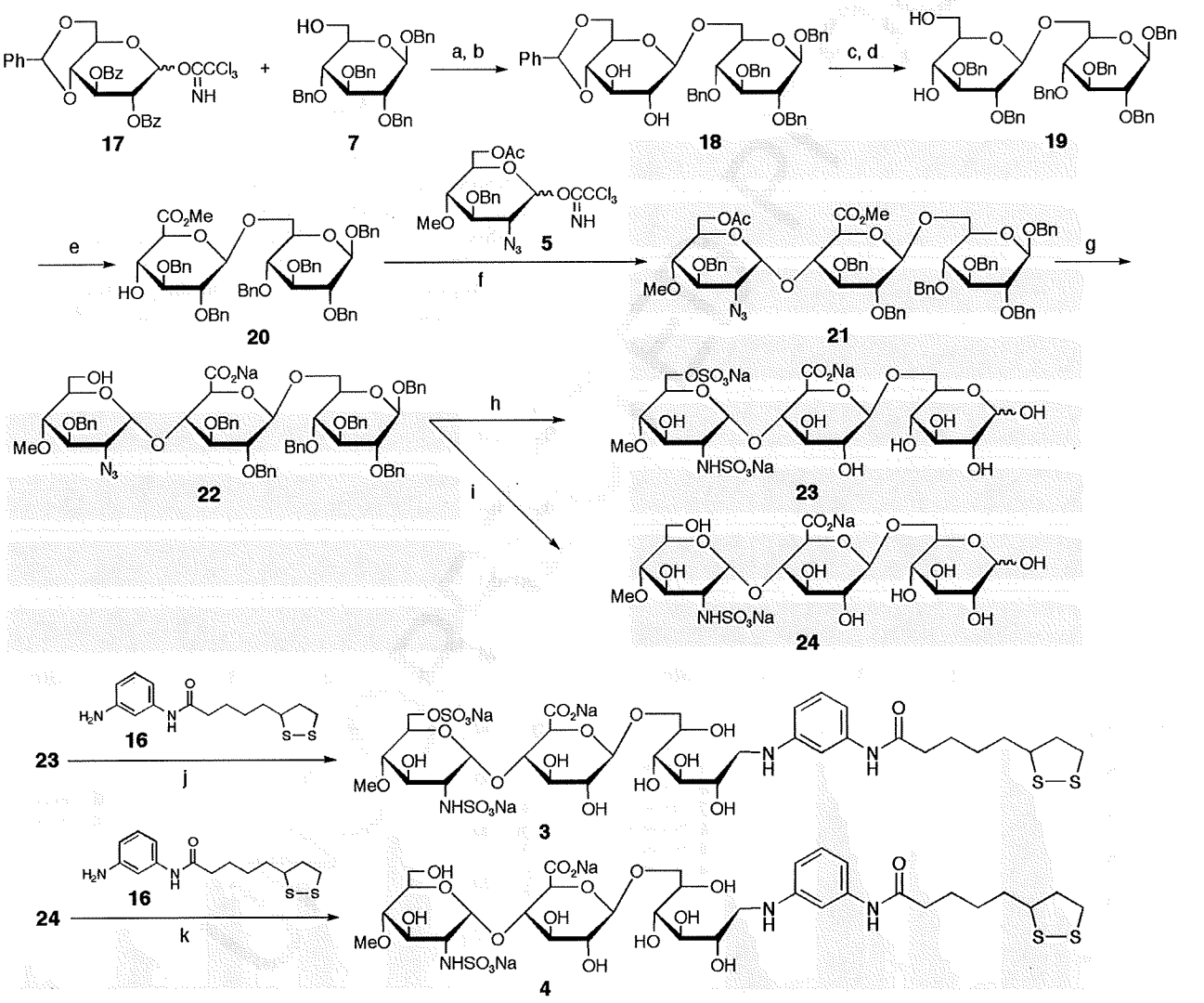

Scheme 2. Synthesis of ligand conjugates **3** and **4** containing GlcNS6S-GlcA and GlcNS-GlcA, respectively. Reagents and conditions: (a) BF_3OEt_2, MS4AP in CH_2Cl_2, −20 °C; (b) 0.1 M NaOMe, 90% (2 steps); (c) NaH, BnBr in DMF, 0 °C → rt, 88%; (d)16% TFA, 8% MeOH in CH_2Cl_2, 0 °C → rt, 93%; (e) TEMPO, KBr, NaClO in CH_2Cl_2; $TMSCHN_2$, 83% (2 steps); (f) TBDMSOTf, MS4AP in toluene, −20 °C, 84%; (g) 5 M NaOH in MeOH/THF (1:1), 89%; (h) SO_3Pyr in Pyr; 10% Pd–C, H_2 (1 kg/cm^2) in THF/H_2O (2:1); SO_3Pyr in H_2O (pH ≈ 9.5); 10% Pd–C, H_2 (7 kg/cm^2) in H_2O/AcOH (5:1), 28% (4 steps); (i) 10% Pd–C, H_2 (1 kg/cm^2) in THF/H_2O (2:1); SO_3Pyr in MeOH/H_2O (3:2); 10% Pd–C, H_2 (7 kg/cm^2) in H_2O/MeOH/AcOH (5:5:2), 39% (3 steps); (j) $NaBH_3CN$ in DMAc/H_2O/AcOH (1:1:0.1), 62%; (k) $NaBH_3CN$ in DMAc/H_2O/AcOH (1:1:0.1), 50%.

Please cite this article in press as: Wakao, M. et al., *Bioorg. Med. Chem. Lett.* (2008), doi:10.1016/j.bmcl.2008.01.069

droxy group was sulfated using sulfur trioxide-pyridine complex at room temperature. After removing the TBDMS group with HFpyridine complex, the azido group was reduced using a catalytic amount of Pd-C under hydrogen atmosphere and the resulting amino group was *N*-sulfated. All benzyl protecting groups were removed by hydrogenolysis using catalytic Pd-C to give the desired trisaccharide **15**. Finally, the reductive amination of trisaccharide **15** with linker compound **16** was performed using $NaBH_3CN$ to afford the desired ligand conjugate **2** in good yield. Compound **2** was purified by gel-filtration chromatography with Sephadex G-25 fine and confirmed by ^1H NMR and ESI-TOF/MS analyses.[13]

The syntheses of ligand conjugates **3** and **4** were carried out in the same fashion as the syntheses of **1** and **2** (Scheme 2). Glycosylation of 6-OH glucose **7** and imidate **17** with trimethylsilyl trifluoromethanesulfonate (TMSOTf) as a promoter and treatment of the resultant with NaOMe gave disaccharide **18** in a good yield. The resulting hydroxy groups of **18** were then protected with a benzyl group. After removal of the benzylidene group, the primary 6′-OH group was selectively oxidized to carboxylic acid using 2,2,6,6-tetramethyl-1-piperidinyloxy (TEMPO).[14] The resulting carboxyl group was esterified with (trimethylsilyl)diazomethane to afford the disaccharide **20**. The 2-azido imidate **5** was condensed with disaccharide **20** using TBDMSOTf at −20 °C to give selectively an α-linked trisaccharide **21**.[11,15] Hydrolysis of the acetyl group and methyl ester was then carried out using aqueous NaOH to give the common intermediate **22** for trisaccharides **23** and **24**. The sulfated trisaccharide **23** was obtained by *O*-sulfation of the 6″-hydoxyl group and reduction and *N*-sulfation of 2′-azido group was followed by hydrogenolysis. Conversely, the sulfated trisaccharide **24** was prepared by the same method as the synthesis of trisaccharide **23**, omitting the *O*-sulfation. The ligand-conjugates **3**[16] and **4**[17] were synthesized in satisfactory yields as similar to the described procedure for compound **2**.

Binding interactions were investigated by use of the SPR imaging sensor.[18] When fibronectin was tested (Fig. 2), specific binding interactions were clearly observed with compounds **1** (GlcNS6S-IdoA2S, K_D = 5.5 nM) and **3** (GlcNS6S-GlcA, K_D = 6.5 nM), but not with compounds **2** (GlcNS-IdoA2S, K_D = 30 nM) and **4** (GlcNS-GlcA, K_D = 33 nM). These results indicate that the *N*-sulfation and 6-*O*-sulfation of glucosamine in HP/HS are important for fibronectin binding, while 2-*O*-sulfation of iduronic acid is less important. Recently,

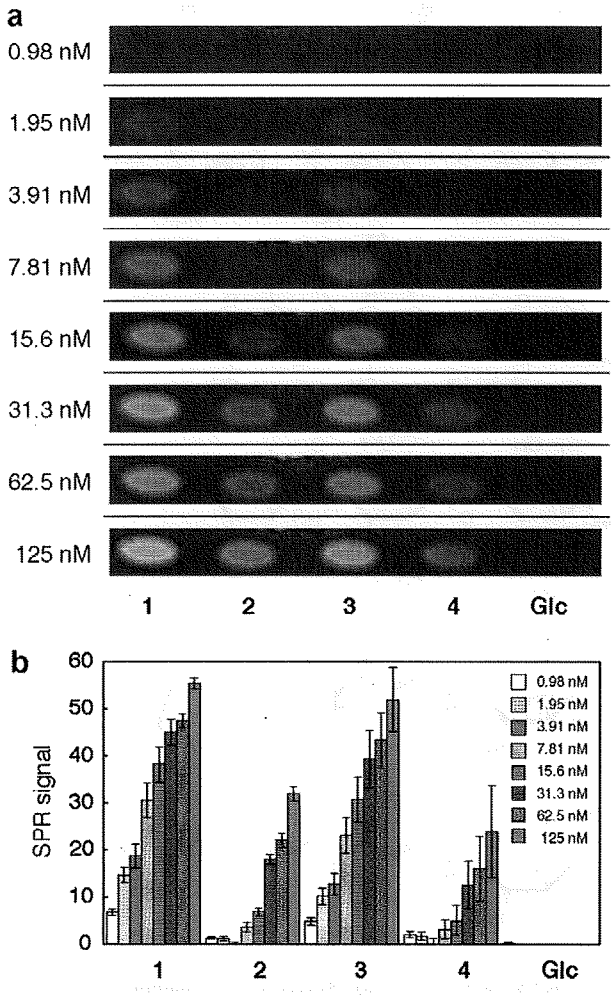

Figure 2. Binding study with fibronectin. (a) SPR difference imaging on the chip immobilized with compounds **1**, **2**, **3**, **4**, and Glcα(1-6)Glc-mono (Glc). Measurements were carried out with analyte in the range between 0.98 and 125 nM. (b) Bar graph profiles of different concentrations of protein. The error bars represent +/− SEM.

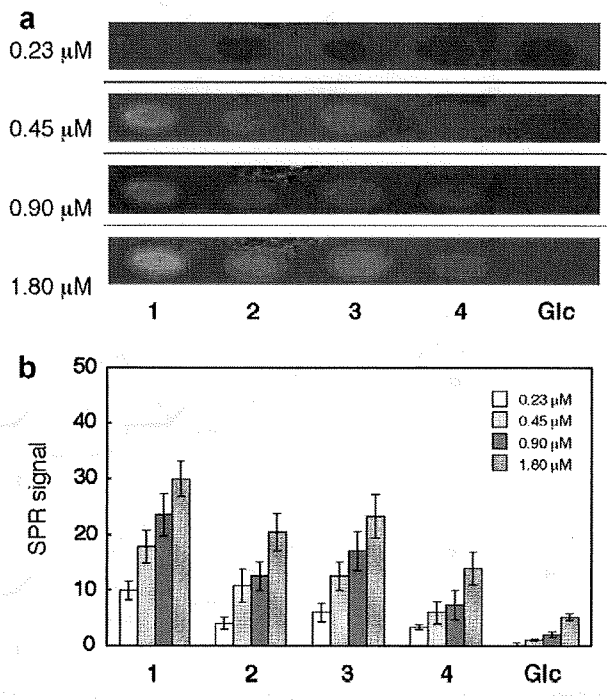

Figure 3. Binding study with rh-vWf-A1. (a) SPR difference imaging on the chip immobilized with compounds **1**, **2**, **3**, **4**, and Glcα(1-6)Glc-mono (Glc). Measurements were carried out with analyte in the range between 0.23 and 1.80 μM. (b) Bar graph profiles of different concentrations. The error bars represent +/− SEM.

Please cite this article in press as: Wakao, M. et al., *Bioorg. Med. Chem. Lett.* (2008), doi:10.1016/j.bmcl.2008.01.069

Couchman and coworkers showed that *N* -sulfation of glucosamine was essential for fibronectin binding and 2-*O*-sulfation of iduonic acid or 6-*O*-sulfation of glucosamine has marginal effects.[19] Additionally, *N*-sulfation and 6-*O*-sulfation of glucosamine were important for focal adhesion formation through syndecan-4, heparan sulfate proteoglycan. Our results are in agreement with those data.

In contrast, when recombinant human vWf A1 domain (rh-vWf-A1)[20] was injected over the chips, a different pattern of oligosaccharide binding preference was noted (Fig. 3). A strong interaction was observed with compounds **1** (GlcNS6S-IdoA2S, K_D = 1.0 μM) and **2** (GlcNS-IdoA2S, K_D = 0.9 μM). Weaker interaction was seen with compound **3** (GlcNS6S-GlcA, K_D = 1.4 μM), while distinctly low binding was observed with compound **4** (GlcNS-GlcA, K_D = 4.3 μM). Although the GlcNS6S-IdoA2S (**1**) disaccharide structure was considered a key binding domain of vWf,[10] the exact disaccharide structure responsible for vWf binding is still unclear. We found previously that clustered compounds containing three units of GlcNS6S-IdoA2S[12] possessed higher competitive binding activity compared to compounds containing less than two units of GlcNS6S-IdoA2S (unpublished data). Together with those data, the current results indicate that the tri-sulfated disaccharide binds vWf best, that loss of either the 6-sulfate of GlcN or the 2-sulfate of Ido reduces vWf binding significantly, and that the *N*-sulfate of GlcN alone is not sufficient for binding vWf.

In conclusion, we have designed new, precisely sulfated oligosaccharides of HP/HS partial structures. These oligosaccharides were efficiently synthesized using appropriate monosaccharide intermediates. Their application in an array type Sugar Chip, using SPR imaging analysis has been shown to be an efficient and specific technology to elucidate the interactions between a protein and multiple sulfated disaccharides, on a real time scale. These techniques can be used for high-throughput screening of protein samples, as well as for solving the structure–function relations of an individual protein–glycosaminoglycan interaction at the molecular and nanoscale.

Acknowledgments

The present work was financially supported in parts by grants from Japan Science and Technology Agency (Pre-venture program to Y.S., CREST to Y.S.), the National Institutes of Health (Grant HL079182 to M.S. and the Department of Veterans Affairs Research Service (to M.S.).

Supplementary data

Supplementary data associated with this article can be found, in the online version, at doi:10.1016/j.bmcl.2008.01.069.

References and notes

1. For reviews, see: (a) Love, K. R.; Seeberger, P. H. *Angew. Chem. Int. Ed.* **2002**, *41*, 3583; (b) Feizi, T.; Fazio, F.; Chai, W.; Wong, C. H. *Curr. Opin. Struct. Biol.* **2003**, *13*, 637; (c) Wang, D. *Proteomics* **2003**, *3*, 2167; (d) Shin, I.; Park, S.; Lee, M. *Chem. Eur. J.* **2005**, *11*, 2894; (e) Ortiz Mellet, C.; Garcia Fernandez, J. M. *ChemBioChem* **2002**, *3*, 819.
2. For articles, see: (a) Blixt, O.; Head, S.; Mandala, T.; Scanlan, C.; Hufflejt, M. E.; Alvarez, R.; Bryan, M. C.; Fazio, F.; Calarese, D.; Stevens, J.; Razi, N.; Stevens, D. J.; Skehel, J. J.; van Die, I.; Burton, D. R.; Wilson, I. A.; Cummings, R.; Bovin, N.; Wong, C. H. *Proc. Natl. Acad. Sci. U.S.A.* **2004**, *101*, 17033; (b) Chevolet, Y.; Martins, J.; Milosevic, N.; Léonard, D.; Zeng, S.; Malissard, M.; Berger, E. G.; Maier, P.; Mathieu, H. J.; Crout, D. H. G.; Sigrist, H. *Bioorg. Med. Chem.* **2001**, *9*, 2943; (c) Park, S.; Lee, M. R.; Pyo, S. J.; Shin, I. *J. Am. Chem. Soc.* **2004**, *126*, 4812; (d) Burn, M. A.; Disney, M. D.; Seeberger, H. P. *ChemBioChem* **2006**, *7*, 421; (e) Houseman, B. T.; Mrksich, M. *Chem. Biol.* **2002**, *9*, 443; (f) Fazio, F.; Bryan, M. C.; Blixt, O.; Paulson, J. C.; Wong, C. H. *J. Am. Chem. Soc.* **2002**, *124*, 14397; (g) Lee, M.; Shin, I. *Angew. Chem. Int. Ed.* **2005**, *44*, 2881; (h) Schwarz, M.; Spector, L.; Gargir, A.; Shtevi, A.; Gortler, M.; Altstock, R. T.; Dukler, A. A.; Dotan, N. *Glycobiology* **2003**, *13*, 749; (i) Zhou, X. C.; Zhou, J. H. *Biosens. Bioelectron.* **2006**, *21*, 1451; (j) Manimala, J. C.; Roach, T. A.; Li, Z. T.; Gildersleeve, J. C. *Angew. Chem. Int. Ed.* **2006**, *45*, 3607; (k) Wang, D.; Liu, S.; Trummer, B. J.; Deng, C. *Nat. Biotechnol.* **2002**, *20*, 275; (l) Chevolet, Y.; Bouillon, C.; Vidal, S.; Morvan, F.; Meyer, A.; Cloarec, J. J.; Jochum, A.; Parly, J. P.; Vasseur, J. J.; Souteyrand, E. *Angew. Chem. Int. Ed.* **2007**, *46*, 2398.
3. Recent carbohydrate chips immobilized sulfated oligosaccharide, see: (a) Suda, Y.; Arano, A.; Fukui, Y.; Koshida, S.; Wakao, M.; Nishimura, T.; Kusumoto, S.; Sobel, M. *Bioconjugate Chem.* **2006**, *17*, 1125; (b) de Paz, J. L.; Noti, C.; Seeberger, P. H. *J. Am. Chem. Soc.* **2006**, *128*, 2766; (c) de Paz, J. L.; Spillmann, D.; Seeberger, P. H. *Chem. Commun.* **2006**, 3116; (d) Noti, C.; de Paz, J. L.; Polito, L.; Seeberger, P. H. *Chem. Eur. J.* **2006**, *12*, 8664; (e) Tully, S. E.; Rawat, M.; Hsieh-Wilson, L. C. *J. Am. Chem. Soc.* **2006**, *128*, 7740.
4. (a) Perou, C. M. *Nature* **2000**, *406*, 747; (b) Ramsey, G. *Nat. Biotechnol.* **1998**, *16*, 40; (c) Marshall, A.; Hodgson, J. *Nat. Biotechnol.* **1998**, *16*, 27; (d) DeRisi, J. L.; Lyer, V. R.; Brown, P. O. *Science* **1997**, *278*, 680.
5. (a) Templin, M. F.; Stoll, D.; Schrenk, M.; Traub, P. C.; Vchringer, C. F.; Joos, T. O. *Trends Biotechnol.* **2002**, *20*, 160; (b) Weinberger, S. R.; Dalmasso, E. A.; Fung, E. T. *Curr. Opin. Chem. Biol.* **2002**, *6*, 86; (c) Fung, E. T.; Thulasiraman, V.; Weinberger, S. R.; Dalmasso, E. A. *Curr. Opin. Biotechnol.* **2001**, *12*, 65; (d) Zhu, H. *Science* **2001**, *293*, 2101; (e) MacBeath, G.; Schreiber, S. L. *Science* **2000**, *289*, 1760.
6. (a) Conrad, H. E. *Heparin-Binding Proteins*; Academic Press: San Diego, 1998; (b) Capila, I.; Lindhardt, R. J. *Angew. Chem. Int. Ed.* **2002**, *41*, 390; (c) Turnbull, J.; Powell, A.; Guimond, S. *Trends Cell Biol.* **2001**, *11*, 75; (d) Bernfield, M.; Götte, M.; Park, P. W.; Reizes, O.; Fitzgerald, M. L.; Lincecum, J.; Zako, M. *Annu. Rev. Biochem.* **1999**, *68*, 729; (e) Rabenstein, D. A. *Nat. Prod. Rep.* **2002**, *19*, 312; (f) Casu, B.; Lindahl, U. *Adv. Carbohydr. Chem. Biochem.* **2001**, *57*, 159.
7. For comprehensive review on the synthesis on GAGs, see: Yeung, B. K. S.; Chong, P. Y. C.; Petillo, P. A. *J. Carbohydr. Chem.* **2002**, *21*, 799.

8. Recent articles, see: (a) Lu, L.-D.; Shie, C.-R.; Kulkarni, S. S.; Pan, G.-R.; Lu, X.-A.; Hung, S.-C. *Org. Lett.* **2006**, *8*, 5995; (b) Zhou, Y.; Lin, F.; Chen, J.; Yu, B. *Carbohydr. Res.* **2006**, *341*, 1619; (c) Codée, J. D. C.; Stubba, B.; Schiattarella, M.; Overkleeft, H. S.; van Boeckel, C. A. A.; van Boom, J. H.; van der Marel, G. A. *J. Am. Chem. Soc.* **2005**, *127*, 3767, And references are therein.
9. (a) Suda, Y.; Marques, D.; Kermode, J. C.; Kusumoto, S.; Sobel, M. *Thromb. Res.* **1993**, *69*, 501; (b) Suda, Y.; Bird, K.; Shiyama, T.; Koshida, S.; Marques, D.; Fukase, K.; Sobel, M.; Kusumoto, S. *Tetrahedron Lett.* **1996**, *37*, 1053.
10. Poletti, L. F.; Bird, K. E.; Marques, D.; Harris, R. B.; Suda, Y.; Sobel, M. *Arterioscler. Thromb. Vasc. Biol.* **1997**, *17*, 925.
11. Koshida, S.; Suda, Y.; Fukui, Y.; Ormsby, J.; Sobel, M.; Kusumoto, S. *Tetrahedron Lett.* **1999**, *40*, 5725.
12. Koshida, S.; Suda, Y.; Sobel, M.; Kusumoto, S. *Tetrahedron Lett.* **2001**, *42*, 1289.
13. Spectral data for compound **2**: ^{1}H NMR (600 MHz, D_2O), δ 7.11 (1 H, t, J = 7.9 Hz), 6.77–6.75 (2 H, m), 6.58 (1H, d, J = 7.9 Hz), 5.22 (1H, d, J = 3.4 Hz), 4.97 (1H, brs), 4.14 (1H, brs), 4.05 (1H, brs), 3.92 (1H, brs), 3.82–3.71 (2H, m), 3.70–3.61 (5H, m), 3.59–3.55 (5H, m), 3.38 (3H, s), 3.28 (1H, dd, J = 9.6 and 3.4 Hz), 3.16 (1H, dd, J = 9.6 and 10.3 Hz), 3.09–3.00 (4H, m), 2.34–2.31 (1H, m), 2.27 (2H, t, J = 6.9), 1.87-1.83 (1H, m), 1.63–1.50 (4H, m), 1.37–1.33 (2H, m), ESI-MS (negative mode); Found: *m/z* 484.62 [(M-3Na+H)$^{2-}$], Calcd. for $C_{33}H_{50}N_3O_{22}S_4Na_3$: 1037.15.
14. (a) Davis, N. J.; Flitsch, S. L. *Tetrahedron Lett.* **1993**, *34*, 1181; (b) Anelli, P. L.; Biffi, C.; Montanari, F.; Quici, S. *J. Org. Chem.* **1987**, *52*, 2559.
15. Kovensky, J.; Duchaussoy, P.; Petitou, M.; Sinaÿ, P. *Tetrahedron: Asymmetry* **1996**, *7*, 3119.
16. Spectral data for compound **3**: ^{1}H NMR (600 MHz, D_2O), δ 7.13 (1H, t, J = 8.2 Hz), 7.11 (1H, s), 6.77 (1H, d, J = 8.2 Hz), 6.60 (1H, d, J = 8.2 Hz), 5.44 (1H, d, J = 3.4 Hz), 4.30 (1H, d, J = 7.6 Hz), 4.15 (1H, d, J = 10.3 Hz), 4.01 (1H, d, J = 10.3 Hz), 3.90 (1H, d, J = 11.0 Hz), 3.83–3.82 (1H, m), 3.76–3.71 (3H, m), 3.66–3.60 (6H, m), 3.52 (1H, dd, J = 10.3 Hz, J = 9.6 Hz), 3.42 (3H, s), 3.27–3.18 (3H, m), 3.14 (1H, dd, J = 3.4 Hz, J = 10.3 Hz), 3.07–3.02 (3H, m), 2.34–2.30 (1H, m), 2.30–2.27 (2H, m), 1.88–1.80 (1H, m), 1.65–1.46 (4H, m), 1.35–1.33 (2H, m), ESI-MS (negative mode); Found: *m/z* 484.65 [(M-3Na+H)$^{2-}$], Calcd. for $C_{33}H_{50}N_3O_{22}S_4Na_3$: 1037.15.
17. Spectral data for compound **4**: ^{1}H NMR (600 MHz, D_2O), δ 7.09 (1H, t, J = 7.9 Hz), 7.04 (1H, s), 6.67 (1H, d, J = 7.9 Hz), 6.52 (1H, d, J = 7.9 Hz), 5.43 (1H, d, J = 4.1 Hz), 4.30 (1H, d, J = 8.2 Hz), 3.91 (1H, d, J = 8.9 Hz), 3.83–3.79 (1H, m), 3.79–3.74 (1H, m), 3.70–3.50 (11H, m), 3.38 (3H, s), 3.25–3.18 (2H, m), 3.14 (1H, dd, J = 9.6 and 9.6Hz), 3.11–2.96 (4H, m), 2.35–2.28 (1H, m), 2.26 (2H, t, J = 6.9 Hz), 1.86–1.80 (1H, m), 1.65–1.45 (4H, m), 1.45–1.27 (2H, m), ESI-MS (negative mode); Found: *m/z* 444.71 [(M-2Na)$^{2-}$], Calcd. for $C_{33}H_{51}N_3O_{19}S_2Na_2$: 935.21.
18. Binding interactions were measured by use of the SPR imaging sensor, Multi SPRinter (TOYOBO Co. Ltd., Osaka, Japan), under the recommended manufacture's guidelines with slight modification. Array-type Sugar Chips were prepared with the purified ligand-conjugates **1**, **2**, **3**, and **4**. An αGlc-containing ligand-conjugate (Glcα4Glc-mono) was also included in the chips as a non-sulfated control. Typical procedures were as follows. After cleaning the chip surface by UV/O_3 treatment, 1 μl of each sample solution (0.5 mM) in H_2O containing 10% glycerol was spotted on the chip by a spotter (TOYOBO), and left to stand overnight at room temperature. The resulting chip was then washed with water, treated with TEG conjugate[21] to mask the unmodified Au surface, and washed with 0.05% Tween 20 aqueous solution and water in an ultrasonic cleaner. A protein solution in PBS containing 0.05% Tween 20 was injected over the surface at a flow rate of 150 μl/min at various concentrations. The binding interaction was monitored at 25 °C as the change in luminance intensity.
19. Mahalingam, Y.; Gallagher, J. T.; Couchman, J. R. *J. Biol. Chem.* **2007**, *282*, 3221.
20. Cruz, M. A.; Handin, H. I.; Wise, R. J. *J. Biol. Chem.* **1993**, *268*, 21238.
21. TEG conjugate is easily prepared by coupling of thioctic acid and 2-{2-[2-(2-hydroxy-ethoxy)-ethoxy]-ethoxy}-ethylamine.

Glycoconj J (2008) 25:269–278
DOI 10.1007/s10719-007-9102-8

Design and synthesis of versatile ganglioside probes for carbohydrate microarrays

Akihiro Imamura · Takeru Yoshikawa · Tatsuya Komori · Masatoshi Ando · Hiromune Ando · Masahiro Wakao · Yasuo Suda · Hideharu Ishida · Makoto Kiso

Received: 2 November 2007 / Revised: 25 December 2007 / Accepted: 26 December 2007 / Published online: 16 January 2008

Abstract A series of ganglioside GM1-, GM2-, and GM3-type probes, in which the ceramide portion is replaced with a glucose residue, were systematically synthesized based on a convergent synthetic method.

Keywords Chemical synthesis · Gangliosides · Glycosylation · Carbohydrate probe

Introduction

Gangliosides, anionic glycosphingolipids with various sugar chains containing one or more residues of sialic acid, exist universally on cell surface. They participate in vital processes, such as immune or nervous systems, as molecules responsible for cell–cell and cell–ligand interactions [1, 2]. In particular, a series of gangliosides, such as GM1, GM2 and GM3, are important as regulatory factors for the differentiation of the central nervous system and serve as cell-attachment receptors for some viruses, bacteria and bacterial toxins [3, 4]. Moreover, many profound relationships between those gangliosides and a number of cancers and diseases have been demonstrated [5, 6]. However, the biological functions of gangliosides are not fully understood, due to their structural complexities and the low affinities of interaction with ligands, despite numerous studies conducted to date. To solve these issues, a considerable number of efforts have gone into the development of analytical techniques for sensitive detection of carbohydrate–ligand interactions. Consequently, many carbohydrate microarray technologies have been developed to facilitate glycomics research [7]. Coincidentally, many carbohydrate probes that incorporate specific functional groups such as azide [8], thiol [9] and maleimide [10] have been chemically synthesized for the fabrication of microarrays. Recently, oligosaccharide-immobilized chips (named Sugar_Chips), which provide real-time and high-throughput analysis of oligosaccharide–protein interaction without any labeling of the targeted protein, have been developed [11], in which chemically synthesized oligosaccharides having D-glucose, which provides a reactive aldehyde functionality, at the reducing end were used. The D-glucose residue also serves as a spacer between a targeted sugar chain and a scaffold for immobilization, because of its appropriate hydrophilicity and flexibility. Furthermore, it has been demonstrated that a reducing sugar directly participates in the noncovalent link to a scaffold [12, 13]. Accordingly, as exemplified in Fig. 1, the chemically synthesized oligo-

A. Imamura (✉) · T. Yoshikawa · T. Komori · M. Ando · H. Ishida · M. Kiso (✉)
Department of Applied Bioorganic Chemistry, Faculty of Applied Biological Sciences, Gifu University, 1-1 Yanagido, Gifu-shi, Gifu 501-1193, Japan
e-mail: gif012@gifu-u.ac.jp
e-mail: kiso@gifu-u.ac.jp

H. Ando
Division of Instrumental Analysis, Life Science Research Center, Gifu University, 1-1 Yanagido, Gifu-shi, Gifu 501-1193, Japan

M. Wakao · Y. Suda
Department of Nanostructure and Advanced Materials, Graduate School of Science and Engineering and Venture Business Laboratory, Kagoshima University, Kohrimoto, Kagoshima 890-0065, Japan

M. Kiso
Institute for Integrated Cell-Material Sciences (iCeMS), Kyoto University, Kyoto, Japan

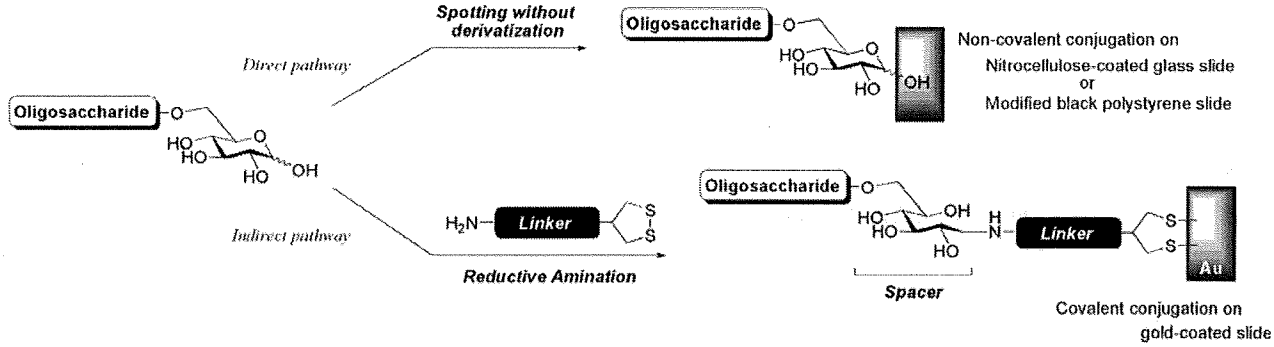

Fig. 1 Two examples for carbohydrate microarray fabrication

saccharide probes are expected to be immobilized by the direct and indirect attachment to scaffolds. We report here the facile synthesis of glucose-ended probes of ganglioside GM1, GM2, and GM3 for carbohydrate microarrays (Fig. 2).

Results and discussion

Taking a look at target molecules, we have hypothetically disconnected them into two parts: common sequence SAα(2→3)Galβ(1→4)Glcβ(1→6)Glc, and the other sugar parts. The common sequence was further disconnected at Galβ(1→4)Glc linkage, providing SAα(2→3)Gal and gentiobiose segments, based on the recently reported efficient syntheses of GM2 analogs [14]. Considering the difficulty to fashion a branch out from galactose residue, the incorporation of GalN parts into Gal residue was planned to be conducted earlier than that of gentiobiose as depicted in Fig. 3.

According to our previous report [14], 2,6-*O*-dibenzylated galactoside was efficiently sialylated at C-3 position with *N*-Troc-protected sialyl donor [15, 16], producing a key sialyl galactoside **4**, which can be obtained in a crystalline form after rough chromatographic purification of the reaction mixture (Fig. 4).

The disaccharide **4** was coupled with Galβ(1→3)GalN **6** [17] or GalN donor **5** in the presence of NIS and TfOH [18] to afford the GM2-core trisaccharide **7** in 97% yield and the GM1-core tetrasaccharide **8** in 89% yield, respectively, as depicted in Table 1.

A series of ganglioside-core frames **4**, **7**, and **8** were converted into the corresponding glycosyl donors **13**, **14**, and **15**, respectively. The selective removal of the Troc group of **4** by the action of zinc–copper couple [19, 20] in acetic acid/1,2-dichloroethane at 40°C proceeded smoothly to give a free amino derivative, which, on successive treatment with acetic anhydride in pyridine afforded the corresponding *N*-acetyl derivative **9**. The use of 1,2-dichloroethane (DCE) was critical for an efficient reduction of Troc group; otherwise the reaction was sluggish. Initially, we were afraid that DCE as solvent itself consumes zinc–copper couple as reductant. Though it is not clear whether DCE is advantageous for electron transfer from zinc–copper couple, we were intriguingly able to observe smooth proceeding of the reaction in a single liquid

Fig. 2 Structure of synthetic ganglioside probes

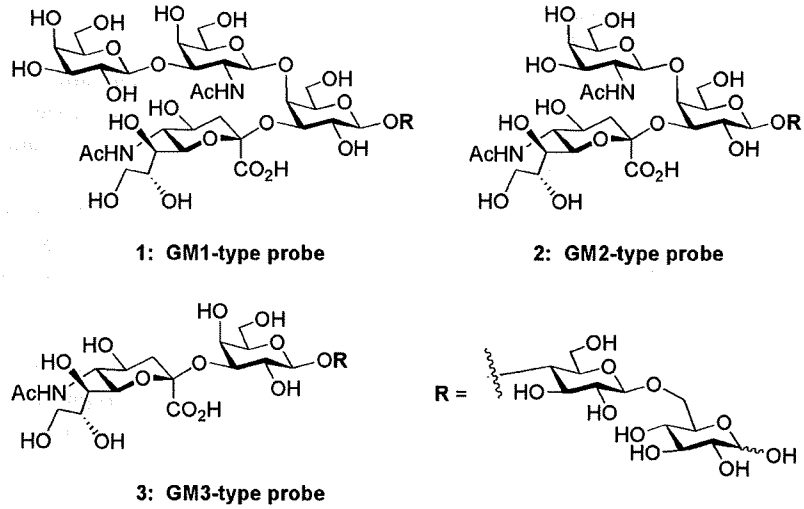

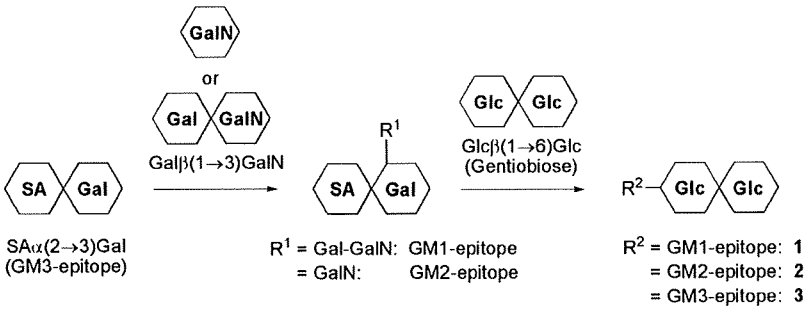

Fig. 3 Systematic reaction scheme for preparation of the reductive glucose-functionalized ganglioside probes

phase within a short time. The cleavage of benzyl groups was executed by hydrogenolysis and the following benzoylation of the resulting hydroxyl groups gave **11**. Libration of the anomeric hydroxyl group of **11** was achieved by treatment with ceric ammonium nitrate (CAN) in acetonitrile–toluene–water (6:5:3) [21]. The obtained hemiacetal was then converted into the β-trichloroacetimidate **13**, which was ready for the final glycosylation with the gentiobiose acceptor **21** as mentioned hereinafter. Interestingly, the use of less than a stoichiometric amount of DBU resulted in the predominant formation of the β-imidate derivative. The conversion of **7** and **8** into the corresponding donor **14** and **15** were also achieved by similar procedure, respectively. (Scheme 1)

Scheme 2 shows the preparation of the gentiobiose acceptor **21** as the common synthetic block, which was expected to have an enhanced reactivity at C-4 hydroxyl due to the effect of electron-donating benzyl groups. Coupling of the known glucose donor **16** [22] and acceptor **17** [23] was conducted in the presence of NIS and TfOH in CH_2Cl_2 at 0°C to give the disaccharide **18** in 90% yield. The β-configuration of the newly formed intersaccharide linkage between **16** and **17** is apparent from the relatively large coupling constant (8.2 Hz) between H-1′ and H-2′ in ^{1}H NMR spectra. Removal of the benzoyl groups under conventional conditions and benzylation of the hydroxyl groups gave **20** with a yield of 88% in two steps. Finally, reductive opening of the benzylidene group was achieved by a treatment with triethylsilane and $BF_3{\cdot}OEt_2$ in CH_2Cl_2 [24] to afford **21** with a yield of 85%.

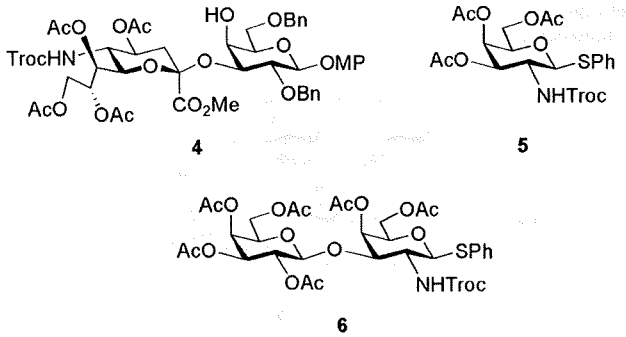

Fig. 4 Structure of glycosyl acceptor (**4**) and donors (**5**, **6**)

Scheme 3 incorporates final glycosylations of **21** with a series of ganglioside-core donors, **13**, **14**, and **15** in the presence of TMSOTf in CH_2Cl_2 at 0°C. The β-imidate **13** was coupled with the gentiobiose acceptor **21** by treatment with TMSOTf at 0°C to afford the desired β-glycoside **22** in an excellent yield. The α-imidate **14** and **15** were subjected to the glycosidation with **21** under essentially the same conditions for **13** to give **23** and **24** in good yields, respectively. Finally, global deprotection of the above-mentioned glycans was conducted. After de-acylation under Zemplén conditions and subsequent saponification of the fully protected oligosaccharides, **24**, **23**, and **22**, hydrogenolysis for each resultant compound was performed in the presence of $Pd(OH)_2/C$ under H_2 atmosphere to afford the target carbohydrate probes **1**, **2** and **3** in good to excellent yields, respectively.

In conclusion, we have succeeded in the synthesis of ganglioside GM1-, GM2-, and GM3-type probes for carbohydrate microarray analyses. It was found that the convergent synthetic strategy between the defined ganglioside-core frame and the reducing end glucose can be used for the synthesis of complex ganglioside probes. In addition, synthesized ganglioside probes are currently used as one of the oligosaccharide probes on immobilized-chips by Suda's group. We are currently underway to expand the existing pool of functional carbohydrate probes containing more complex gangliosides.

Experimental

General procedures

All reactions were carried out under a positive pressure of argon, unless otherwise noted. All chemicals were purchased from commercial suppliers and used without further purification, unless otherwise noted. Molecular sieves were purchased from Wako Chemicals Inc. and dried at 300°C for 2 h in muffle furnace prior to use. ^{1}H NMR and ^{13}C NMR spectra were recorded with a Varian Inova 400/500 spectrometer and a JEOL ECA 500/600 spectrometer. Chemical shifts are reported in parts per million (ppm) downfield from tetramethylsilane. Data are presented as

Table 1 Glycosylation of **4** with glycosyl donors **5** and **6**

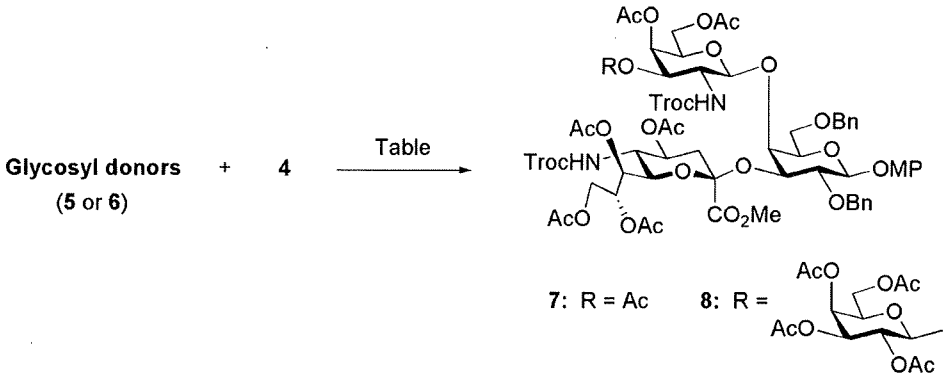

Entry	Donor	Condition	Temp.[°C]	Product	% Yield
1	**5**	NIS TfOH MS4Å CH_2Cl_2	0	**7**	97
2	**6**		-40	**8**	89

follows: Chemical shift, multiplicity (s=singlet, d=doublet, t=triplet, dd=double of doublet, m=multiplet and/or multiple resonances), integration, coupling constant in Hertz (Hz). MALDI-TOF MS spectra were recorded in the positive ion mode on a Bruker Autoflex with the use of α-cyano-4-hydroxy-cinnamic acid (CHCA) as a matrix. Optical rotations were measured with a 'Horiba SEPA-300' polarimeter. Column chromatography was performed on silica gel (Fuji Silysia Co., 80 and 300 mesh). Reactions were monitored by TLC on silica gel $60F_{254}$ (Merck, glass plate) and the compounds were detected by examination under UV light (2,536 Å) and visualized by dipping the plates in a 10% sulfuric acid–ethanol solution or 20% phosphomolybdic acid–ethanol solution followed by heating. Organic solutions were concentrated by rotary evaporation below 45°C under reduced pressure. Solvent systems in chromatography were specified in *v/v*.

4-Methoxyphenyl {methyl 5-acetamido-4,7,8,9-tetra-O-acetyl-3,5-dideoxy-D-glycero-α-D-galacto-2-nonulopyranosylonate-(2→3)}-4-O-acetyl-2,6-di-O-benzyl-β-D-galactopyranoside (**9**) To a solution of compound **4** (500 mg, 465 μmol) in 1,2-dichloroethane (6.1 ml) were added acetic acid (18.3 ml) and zinc–copper couple (2.50 g). The mixture was stirred for 1.5 h at 40°C, as the proceeding of the reaction was monitored by TLC ($CHCl_3$/MeOH=15:1). The

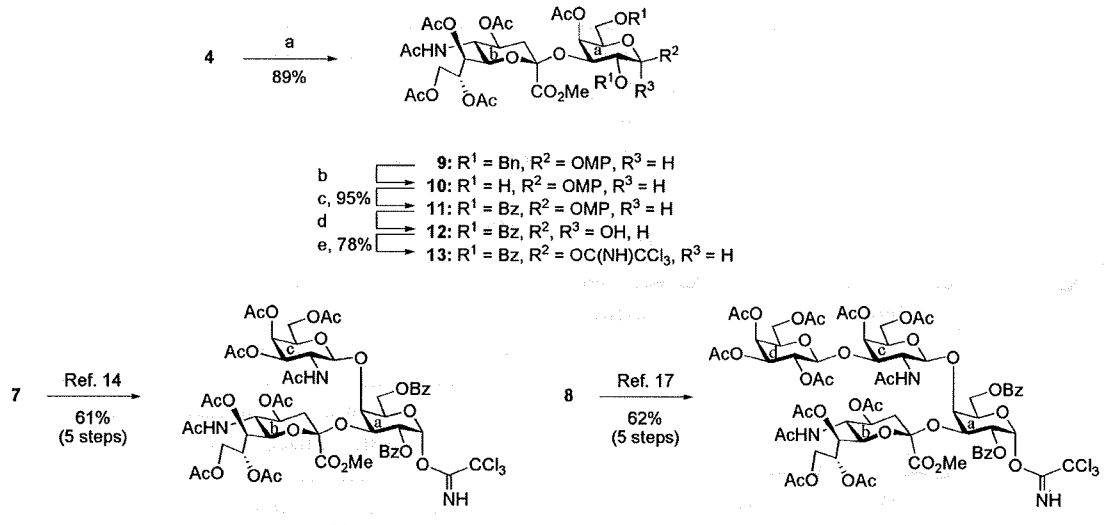

Scheme 1 Conversion of ganglioside-core frames to the corresponding glycosyl donors. Reagents and conditions: *a* Zn-Cu, AcOH, 1,2-DCE, 40°C then Ac_2O, Py; *b* $Pd(OH)_2/C$, H_2, EtOH; *c* Bz_2O, Py; *d* CAN, CH_3CN-PhMe-H_2O (6/5/3); *e* CCl_3CN, DBU, CH_2Cl_2, 0°C

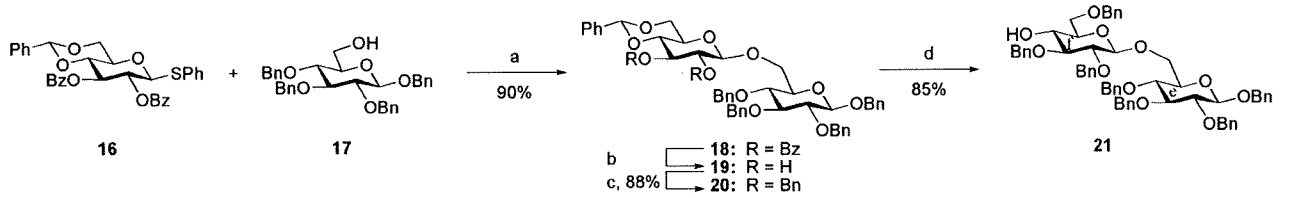

Scheme 2 Preparation of the gentiobiosyl acceptor **21**. Reagents and conditions: *a* NIS, TfOH, MS4Å, CH_2Cl_2, 0°C; *b* NaOMe, MeOH-THF (2/1); *c* BnBr, NaH, DMF; *d* TESH, $BF_3{\cdot}OEt_2$, CH_2Cl_2

reaction mixture was filtered through Celite. The combined filtrate and washings was extracted with $CHCl_3$, and the organic layer was washed with H_2O, sat. Na_2CO_3, and brine, dried over Na_2SO_4 and concentrated. To a solution of the residue in pyridine (5.0 ml) was added acetic anhydride (2.5 ml). The mixture was stirred for 13 h at ambient temperature, as the proceeding of the reaction was monitored by TLC ($CHCl_3$/MeOH=15:1). The reaction mixture was coevaporated with toluene and extracted with $CHCl_3$. The organic layer was washed with 2 M HCl, H_2O, sat. $NaHCO_3$ and brine, dried over Na_2SO_4 and concentrated. The residue was purified with column chromatography on silica gel (EtOAc/hexane=3:1) to give **9** (406 mg, 89%).; $[\alpha]_D$=−15.4° (*c* 0.9, $CHCl_3$); ^{1}H-NMR (600 MHz, $CDCl_3$): δ 7.45–6.77 (m, 14 H, 2 Ph and 1 MP), 5.53 (m, 1 H, H-8b), 5.33 (dd, 1 H, H-7b), 5.24 (d, 1 H, $J_{5,NH}$=8.9 Hz, NH), 5.07 (m, 2 H, H-1a, 4a), 4.96–4.88 (m, 3 H, H-4b, 2 CH*H*Ph), 4.63 (dd, 1 H, H-3a), 4.53 (d, 1 H, CH*H*Ph), 4.46 (d, 1 H, CH*H*Ph) 4.36 (dd, 1 H, H-9'b), 4.13 (q, 1 H, $J_{5,NH}$= 8.9 Hz, H-5b), 3.96–3.94 (m, 2 H, H-6'a, 9b), 3.85 (s, 3 H, OMe), 3.76–3.73 (m, 5 H, H-2a, 6b, OMe), 3.56–3.52 (m, 2 H, H-5a, 6a), 2.63 (dd, 1 H, H-3b$_{eq}$), 2.12–1.83 (m, 19 H,6 Ac, H-3b$_{ax}$); ^{13}C-NMR (100 MHz, $CDCl_3$) δ 170.9, 170.6, 170.3, 170.2, 170.0, 168.1, 155.1, 151.7, 139.4, 138.0, 128.3, 128.1, 127.7, 127.6, 127.1, 118.2, 114.4, 102.4, 97.1, 78.1, 74.8, 73.5, 73.1, 72.3, 72.2, 69.5, 68.9, 68.7, 68.6, 67.2, 62.2, 55.6, 53.1, 49.2, 37.6, 23.2, 21.3, 20.8, 20.8, 20.5; MALDI MS: *m/z*: calcd for $C_{49}H_{59}O_{20}NNa$: 1,004.35; found: 1,004.35 $[M + Na]^+$.

4-Methoxyphenyl {methyl 5-acetamido-4,7,8,9-tetra-O-acetyl-3,5-dideoxy-D-glycero-α-D-galacto-2-nonulopyranosylonate-(2→3)}-4-O-acetyl-2,6-di-O-benzoyl-β-D-galactopyranoside (**11**) To a solution of compound **9** (385 mg, 392 μmol) in EtOH (30 ml) was added palladium hydroxide [$Pd(OH)_2$] (20 wt% Pd on carbon; 400 mg). The mixture was vigorously stirred for 4 h at ambient temperature under hydrogen atmosphere, as the proceeding of the reaction was monitored by TLC ($CHCl_3$/MeOH=15:1). The reaction mixture was filtered through Celite. The combined filtrate and washings was concentrated. To a solution of the residue in pyridine (5.0 ml) was added benzoic anhydride (354 mg, 1.57 mmol). The mixture was stirred for 16 h at ambient temperature, as the proceeding of the reaction was monitored by TLC ($CHCl_3$/MeOH=15:1). The reaction mixture was coevaporated with toluene and extracted with $CHCl_3$. The organic layer was washed with 2 M HCl, H_2O, sat. $NaHCO_3$ and brine, dried over Na_2SO_4 and concentrated. The residue was purified with column chromatography on silica gel (EtOAc/hexane=3:1) to give **11** (380 mg, 95%); $[\alpha]_D$=+ 27.9° (*c* 4.2, $CHCl_3$); ^{1}H-NMR (600 MHz, $CDCl_3$): δ 8.17–6.67 (m, 14 H, 2 Ph and 1 MP), 5.59 (m, 1 H, H-8b), 5.55 (t, 1 H, $J_{1,2}$=8.3 Hz, $J_{2,3}$=10.3 Hz, H-2a), 5.26 (d, 1 H, $J_{1,2}$=8.3 Hz, H-1a), 5.20 (dd, 1 H, $J_{6,7}$=2.8 Hz, H-7b), 5.16 (d, 1 H, $J_{3,4}$=3.4 Hz, H-4a), 5.14 (d, 1 H, NH), 4.87 (dd, 1 H, $J_{2,3}$=10.3 Hz, $J_{3,4}$=3.4 Hz, H-3a), 4.85 (m, 1 H, H-4b), 4.46 (t, 1 H, H-6'a), 4.35 (dd, 1 H, H-6a), 4.27 (dd, 1 H, H-9'b), 4.19 (t, 1 H, H-5b), 3.91 (dd, 1 H, H-9b), 3.86–3.79 (m, 4 H, H-5b, OMe) 3.71 (s, 3 H, OMe), 3.61 (dd, 1 H, $J_{6,7}$=2.8 Hz,

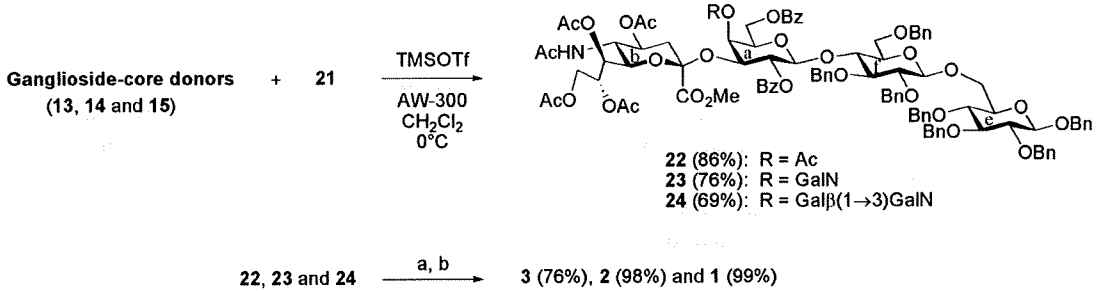

Scheme 3 Coupling of the ganglioside-core donors (**13**, **14** and **15**) and the gentiobioside acceptor (**21**), and subsequent global deprotections. Reagents and conditions: *a* NaOMe, MeOH, 45°C or reflux, then H_2O; (b) $Pd(OH)_2$/C, H_2, H_2O or MeOH-H_2O (5/2), RT or 40°C

H-6b), 2.59 (dd, 1 H, H-3b$_{eq}$), 2.19–1.44 (m, 19 H, 6 Ac, H-3b$_{ax}$); ^{13}C-NMR (100 MHz, $CDCl_3$) δ 170.7, 170.6, 170.3, 170.2, 170.0, 168.0, 165.7, 165.3, 155.4, 151.3, 133.2, 133.0, 130.1, 130.0, 129.7, 128.3, 128.3, 118.9, 114.2, 101.1, 96.7, 71.6, 71.1, 70.8, 69.3, 67.6, 67.4, 66.4, 62.3, 62.0, 55.4, 53.0, 48.7, 37.2, 23.2, 21.3, 20.7, 20.1; MALDI MS: *m/z*: calcd for $C_{49}H_{55}O_{22}NNa$: 1,032.31; found: 1,032.38 [*M* + Na]$^+$.

{Methyl 5-acetamido-4,7,8,9-tetra-O-acetyl-3,5-dideoxy-D-glycero-α-D-galacto-2-nonulopyranosylonate-(2→3)}-4-O-acetyl-2,6-di-O-benzoyl-β-D-galactopyranosyl Trichloroacetimidate (**13**) To a solution of compound **11** (164 mg, 162 μmol) in mixed solvent (MeCN/PhMe/H_2O= 3.5:2.9:1.7 ml) was added diammonium cerium(IV) nitrate (CAN; 445 mg, 812 μmol). The mixture was stirred for 5 h at ambient temperature, as the proceeding of the reaction was monitored by TLC ($CHCl_3$/MeOH=20:1). The reaction mixture was extracted with $CHCl_3$, and the organic layer was washed with H_2O, sat. $NaHCO_3$ and brine, dried over Na_2SO_4 and concentrated. The residue was purified with column chromatography on silica gel ($CHCl_3$/MeOH= 65:1) to give **12** (147 mg). To a solution of compound 12 in CH_2Cl_2 (5.0 ml) were added trichloroacetonitrile (410 μl, 407 μmol) and 1,8-diazabicyclo[5.4.0]-7-undecene (DBU; 4.9 μl, 33.0 μmol). The mixture was stirred for 2 h at 0°C, as the proceeding of the reaction was monitored by TLC ($CHCl_3$/MeOH=20:1). The reaction mixture was concentrated and the residue was purified with column chromatography on silica gel ($CHCl_3$/MeOH=75:1) to give **13** (132 mg, 78%).; $[\alpha]_D$=+ 18.6° (*c* 0.8, $CHCl_3$); ^{1}H-NMR (600 MHz, $CDCl_3$): δ 8.67 (s, 1 H, C=NH), 8.10–7.41 (m, 10 H, 2 Ph), 6.20 (d, 1 H, $J_{1,2}$=8.3 Hz, H-1a), 5.60–5.56 (m, 2 H, H-2a, H-8b), 5.22–5.20 (m, 2 H, H-4a, H-7b), 4.98 (d, 1 H, $J_{5,NH}$=10.3 Hz, NH-b), 4.93 (dd, 1 H, H-3a), 4.87 (m, 1 H, H-4b), 4.49 (q, 1 H, H-6'a), 4.34–4.29 (m, 3 H, H-5a, 6a, 9'b), 3.93 (dd, 1 H, H-9b), 3.85–3.77 (m, 4 H, H-5b, OMe), 3.60 (dd, 1 H, H-6b), 2.58 (dd, 1 H, H-3b$_{eq}$), 2.19–1.43 (m, 19 H, 6 Ac, H-3b$_{ax}$); ^{13}C-NMR (100 MHz, $CDCl_3$) δ 170.8, 170.7, 170.6, 170.2, 170.2, 170.0, 168.0, 165.7, 165.1, 161.1, 133.2, 130.1, 129.9, 129.7, 129.7, 128.3, 128.3, 96.8, 96.4, 90.3, 77.2, 71.8, 71.5, 71.1, 70.0, 69.4, 67.6, 67.4, 66.5, 62.4, 61.5, 53.1, 48.8, 37.3, 29.7, 23.1, 21.4, 20.8, 20.7, 20.2; MALDI MS: *m/z*: calcd for $C_{44}H_{49}O_{21}N_2Cl_3Na$: 1,069.18; found: 1,069.41 [*M* + Na]$^+$.

Benzyl 2,3-di-O-benzoyl-4,6-O-benzylidene-β-D-glucopyranosyl-(1→6)-2,3,4-tri-O-benzyl-β-D-glucopyranoside (**18**) To a solution of compound **16** (970 mg, 1.70 mmol) and **17** (762 mg, 1.41 mmol) in CH_2Cl_2 (31 ml) was added molecular sieves 4 Å (1.70 g). The suspension was stirred for 2 h and cooled to 0°C. To the mixture were added *N*-iodosuccinimide (NIS; 765 mg, 3.40 mmol) and trifluoromethanesulfonic acid (TfOH) (30 μl, 0.34 mmol) and stirring was continued for 1.5 h. Completion of the reaction was confirmed by TLC (EtOAc/hexane=1:3). The reaction mixture was filtered through Celite. The combined filtrate and washings was extracted with $CHCl_3$, and the organic layer was washed with sat. Na_2CO_3, sat. $Na_2S_2O_3$ and brine, dried over Na_2SO_4 and concentrated. The residue was purified with column chromatography on silica gel (EtOAc/hexane=1:5) to give **18** (1.26 g, 90%).; $[\alpha]_D$=-9.3° (*c* 1.0, $CHCl_3$); ^{1}H-NMR (600 MHz, $CDCl_3$): δ 7.95–7.13 (m, 35 H, 7 Ph), 5.75 (t, 1 H, $J_{2,3}$=8.8 Hz, $J_{3,4}$=8.6 Hz, H-3f), 5.55 (s, 1 H, >C*H*Ph), 5.52 (t, 1 H, $J_{1,2}$=8.2 Hz, $J_{2,3}$=8.8 Hz, H-2f), 4.91–4.86 (m, 3 H, H-1f, 2 CH*H*Ph), 4.77–4.65 (m, 4 H, 4 CH*H*Ph), 4.49–4.39 (m, 4 H, H-1e, 6f, 2 CH*H*Ph), 4.14 (d, 1 H, J_{gem}= 11.0 Hz, H-6e), 3.99 (t, 1 H, $J_{3,4}$=8.6 Hz, $J_{4,5}$=9.6 Hz, H-4f), 3.89 (br t, 1 H, J_{gem}=10.3 Hz, $J_{5,6}$=9.3 Hz, H-6'f), 3.73–3.63 (m, 2 H, H-6'e, 5f), 3.57 (t, 1 H, $J_{2,3}$=8.4 Hz, H-3e), 3.45–3.40 (m, 3 H, H-2e, 4e, 5e); ^{13}C-NMR (150 MHz, $CDCl_3$) δ 165.7, 165.2, 138.6, 138.5, 138.1, 137.5, 137.0, 133.3, 133.2, 129.9, 129.8, 129.5, 129.3, 129.1, 128.5, 128.4, 128.3, 128.1, 128.0, 127.9, 127.8, 127.7, 127.6, 126.3, 102.5, 101.6, 101.4, 84.7, 82.2, 78.8, 77.8, 75.7, 75.0, 74.9, 74.7, 72.7, 72.3, 71.1, 68.8, 68.4, 67.2, 66.6, 29.8; MALDI MS: *m/z*: calcd for $C_{61}H_{58}O_{13}Na$: 1,021.38; found: 1,021.49 [*M* + Na]$^+$.

Benzyl 2,3-di-O-benzyl-4,6-O-benzylidene-β-D-glucopyranosyl-(1→6)-2,3,4-tri-O-benzyl-β-D-glucopyranoside (**20**) To a solution of compound **18** (1.25 g, 1.25 mmol) in mixed solvent (MeOH/THF=15:7.5 ml) was added sodium methoxide (28% in MeOH; 24 mg). The mixture was stirred for 7.5 h at ambient temperature, as the proceeding of the reaction was monitored by TLC ($CHCl_3$/MeOH= 50:1). The reaction mixture was neutralized with Dowex (H^+) and filtered through cotton. The combined filtrate and washings was concentrated under diminished pressure. To a solution of the residue in DMF (12.5 ml) were added sodium hydride 60% (200 mg, 5.00 mmol) and benzyl bromide (594 μl, 5.00 mmol). The mixture was stirred for 3 h at ambient temperature, as the proceeding of the reaction was monitored by TLC (toluene/EtOAc= 12:1). Triethylamine and ammonium chloride were added to the reaction mixture. The reaction mixture was washed with H_2O and brine, dried over Na_2SO_4 and concentrated. The residue was purified with column chromatography on silica gel (toluene/EtOAc=40:1) to give **20** (1.07 g, 88%).; $[\alpha]_D$=−21.7° (*c* 1.1, $CHCl_3$); ^{1}H-NMR (600 MHz, $CDCl_3$): δ 7.49–7.21 (m, 35 H, 7 Ph), 5.56 (s, 1 H, >C*H*Ph), 4.96–4.69 (m, 10 H, 10 CH*H*Ph), 4.59 (d, 1 H, $J_{1,2}$=8.2 Hz, H-1f), 4.54–4.45 (m, 3 H, H-1e, 2 CH*H*Ph), 4.33 (dd, 1 H, J_{gem}=9.3 Hz, $J_{5,6}$=4.8 Hz, H-6f), 4.16 (d, 1 H, J_{gem}=11.0 Hz, H-6e), 3.79–3.72 (m, 2 H, H-6'e, 6'f), 3.68–3.64 (m, 3 H, H-2f, 4f, 5f), 3.57 (t, 1 H, $J_{2,3}$=8.5 Hz, $J_{3,4}$=9.0 Hz, H-3e), 3.50–3.47 (m, 2 H, H-2e, 2f), 3.44 (t,

1 H, $J_{3,4}$=9.6 Hz, $J_{4,5}$=9.6 Hz, H-4e), 3.35 (m, 1 H, H-5e); ^{13}C-NMR (150 MHz, $CDCl_3$) δ 138.6, 138.6, 138.8, 138.1, 137.6, 137.5, 129.1, 128.7, 128.5, 128.4, 128.3, 128.3, 128.3, 128.2, 128.1, 128.0, 128.0, 127.9, 127.8, 127.8, 127.7, 127.6, 126.1, 104.3, 102.7, 101.3, 84.8, 82.4, 82.1, 81.6, 81.0, 78.3, 77.3, 75.8, 75.4, 75.2, 75.1, 74.9, 71.3, 68.9, 66.1, 29.8; MALDI MS: *m/z*: calcd for $C_{61}H_{62}O_{11}Na$: 993.42; found: 993.50 $[M + Na]^+$.

Benzyl 2,3,6-tri-O-benzyl-β-D-glucopyranosyl-(1→6)-2,3,4-tri-O-benzyl-β-D-glucopyranoside (**21**) To a solution of compound **20** (82 mg, 84.5 μmol) in CH_2Cl_2 (845 μl) were added triethylsilane (162 μl, 1.01 mmol) and boron trifluoride diethyl etherate (BF_3·OEt_2; 21.4 μl, 169 μmol). The mixture was stirred for 1.5 h at ambient temperature, as the proceeding of the reaction was monitored by TLC (toluene/EtOAc=12:1). The reaction mixture was diluted with $CHCl_3$ and washed with sat. $NaHCO_3$, H_2O and brine, dried over Na_2SO_4 and concentrated. The residue was purified with column chromatography on silica gel (toluene/EtOAc=20:1) to give **21** (70 mg, 85%).; $[\alpha]_D$=−12.9° (*c* 1.0, $CHCl_3$); ^{1}H-NMR (600 MHz, $CDCl_3$): δ 7.35–7.21 (m, 35 H, 7 Ph), 5.01–4.69 (m, 10 H, 10 CH*H*Ph), 4.59–4.51 (m, 3 H, H-1f, 2 CH*H*Ph), 4.46 (d, 1 H, $J_{1,2}$=9.6 Hz, H-1e), 4.19 (d, 1 H, J_{gem}=11.0 Hz, H-6e), 3.74–3.58 (m, 6 H, H-6′e, 3f, 4f, 5f, 6f, 6′f), 3.50–3.39 (m, 5 H, H-2f, 2e, 3e, 4e, 5e), 2.54 (s, 1 H, -OH); ^{13}C-NMR (150 MHz, $CDCl_3$) δ 138.9, 138.7, 138.5, 138.5, 138.2, 138.0, 137.6, 128.6, 128.5, 128.5, 128.4, 128.3, 128.2, 128.1, 128.0, 128.0, 127.9, 127.8, 127.7, 104.1, 102.7, 84.8, 84.2, 82.4, 81.6, 78.4, 77.3, 75.8, 75.4, 75.3, 75.1, 74.9, 74.8, 74.1, 73.8, 71.8, 71.3, 68.8, 29.8; MALDI MS: *m/z*: calcd for $C_{61}H_{64}O_{11}Na$: 995.43; found: 995.38 $[M + Na]^+$.

Benzyl {methyl 5-acetamido-4,7,8,9-tetra-O-acetyl-3,5-dideoxy-D-glycero-α-D-galacto-2-nonulopyranosylonate-(2→3)}-4-O-acetyl-2,6-di-O-benzoyl-β-D-galactopyranosyl-(1→4)-2,3,6-tri-O-benzyl-β-D-glucopyranosyl-(1→6)-2,3,4-tri-O-benzyl-β-D-glucopyranoside (**22**) To a solution of compound **13** (107 mg, 102 μmol) and **21** (200 mg, 206 μmol) in CH_2Cl_2 (5.0 ml) was added molecular sieves 4 Å (1.00 g). The suspension was stirred for 1 h and cooled to 0°C. To the mixture was added trimethylsilyl trifluoromethanesulfonate (TMSOTf; 3.7 μl, 20 μmol) and stirring was continued for 1 h. Completion of the reaction was confirmed by TLC ($CHCl_3$/MeOH=20:1). The reaction mixture was filtered through Celite. The combined filtrate and washings was extracted with $CHCl_3$, and the organic layer was washed with sat. Na_2CO_3 and brine, dried over Na_2SO_4 and concentrated. The residue was purified with column chromatography on silica gel ($CHCl_3$/MeOH=75:1) to give **22** (170 mg, 86%).; $[\alpha]_D$=+ 2.0° (*c* 0.5, $CHCl_3$); ^{1}H-NMR (500 MHz, $CDCl_3$): δ 8.24–7.15 (m, 45 H, 9 Ph), 5.66 (m, 1 H, H-8b), 5.31 (t, 1 H, $J_{1,2}$=8.0 Hz, $J_{2,3}$= 9.7 Hz, H-2a), 5.18 (dd, 1 H, H-7b), 5.13 (d, 1 H, $J_{1,2}$=8.0 Hz, H-1a), 5.06 (d, 1 H, $J_{3,4}$=3.4 Hz, H-4a), 4.99 (d, 1 H, CH*H*Ph), 4.92–4.66 (m, 12 H, H-3a, 4b, NH, 9 CH*H*Ph), 4.49–4.36 (m, 7 H, H-6′a, 1e, 1f, 4 CH*H*Ph), 4.29 (d, 1 H, H-9′b), 4.13–3.88 (m, 6 H, H-5a, 6a, 5b, 9b, H-6′ of Glc units), 3.77 (q, 1 H, H-5b), 3.71 (s, 1 H, OMe), 3.67–3.35 (m, 10 H, H-6b, Glc units), 3.22 (m, 1 H, H-5 of Glc units), 2.52 (dd, 1 H, J_{gem}=12.6 Hz, $J_{3eq,4}$=4.6 Hz H-3b$_{eq}$), 2.13–1.43 (m, 19 H, 6 Ac, H-3b$_{ax}$) ^{13}C-NMR (125 MHz, $CDCl_3$) δ 170.8, 170.7, 170.3, 170.2, 170.1, 168.0, 165.4, 165.1, 139.1, 138.6, 138.4, 138.0, 137.6, 133.3, 133.0, 130.3, 130.0, 129.8, 129.7, 128.6, 128.4, 128.3, 128.3, 128.2, 128.1, 128.1, 127.9, 127.9, 127.7, 127.6, 127.4, 127.3, 127.2, 127.1, 103.7, 102.7, 100.4, 96.9, 84.7, 82.9, 82.3, 81.6, 78.2, 76.3, 75.7, 75.2, 75.1, 74.9, 74.8, 74.8, 74.4, 72.8, 71.7, 71.5, 71.2, 70.4, 69.4, 69.0, 68.5, 67.4, 67.0, 66.5, 62.5, 61.2, 53.0, 48.8, 37.3, 29.7, 23.2, 21.3, 20.8, 20.7, 20.7, 20.3; MALDI MS: *m/z*: calcd for $C_{103}H_{111}O_{31}NNa$: 1,880.70; found: 1,880.96 $[M + Na]^+$.

Benzyl 2-acetamido-3,4,6-tri-O-acetyl-2-deoxy-β-D-galactopyranosyl-(1→4)-{methyl 5-acetamido-4,7,8,9-tetra-O-acetyl-3,5-dideoxy-D-glycero-α-D-galacto-2-nonulopyranosylonate-(2→3)}-2,6-di-O-benzoyl-β-D-galactopyranosyl-(1→4)-2,3,6-tri-O-benzyl-β-D-glucopyranosyl-(1→6)-2,3,4-tri-O-benzyl-β-D-glucopyranoside (**23**) To a solution of compound **14** (58 mg, 43 μmol) and **21** (84 mg, 86 μmol) in CH_2Cl_2 (2.0 ml) was added molecular sieves 4 Å (165 mg). The suspension was stirred for 1 h at ambient temperature and cooled to 0°C. To the mixture was added TMSOTf (1.6 μL, 8.6 μmol) and stirring was continued for 3.5 h. Completion of the reaction was confirmed by TLC ($CHCl_3$/MeOH=15:1). Triethylamine was then added to quench the reaction. The reaction mixture was filtered through Celite. The combined filtrate and washings was extracted with $CHCl_3$, and the organic layer was washed with sat. $NaHCO_3$ and brine, dried over Na_2SO_4 and concentrated. The residue was purified with column chromatography on silica gel ($CHCl_3$/MeOH=50:1) to give **23** (70 mg, 76%).; $[\alpha]_D$=−11.0° (*c* 0.76, $CHCl_3$); ^{1}H-NMR (600 MHz, $CDCl_3$): δ 8.01–7.15 (m, 45 H, 9 Ph), 5.97 (d, 1 H, NH-c), 5.49 (dd, 1 H, $J_{3,4}$=2.7 Hz, H-3c), 5.40 (m, 1 H, H-8b), 5.37 (d, 1 H, $J_{3,4}$=2.7 Hz, H-4c), 5.34 (t, 1 H, $J_{1,2}$= 10.2 Hz, H-2a), 5.25 (d, 1 H, H-7b), 5.14 (br d, 1 H, NH-b), 5.06 (d, 1 H, $J_{1,2}$=8.9 Hz, H-1c), 5.00 (dt, 1 H, $J_{3eq,4}$= 4.8 Hz, H-4b), 4.95–4.88 (m, 4 H, 4 CH*H*Ph), 4.82–4.80 (m, 3 H, 3 CH*H*Ph), 4.79 (d, 1 H, $J_{1,2}$=10.2 Hz, H-1a), 4.72 (t, 2 H, 2 CH*H*Ph), 4.67 (d, 1 H, CH*H*Ph), 4.62 (q, 1 H, H-6c), 4.51 (d, 1 H, CH*H*Ph), 4.47 (d, 1 H, CH*H*Ph), 4.43 (d, 1 H, CH*H*Ph), 4.40 (d, 1 H, $J_{1,2}$=8.2 Hz, H-1f), 4.37 (d, 1 H, $J_{1,2}$= 8.2 Hz, H-1e), 4.28 (d, 1 H, CH*H*Ph), 4.19 (t, 1 H, H-5a), 4.15–3.96 (m, 10 H, H-3a, 4a, 6a, 6′a, 5b, 9b, 9′b, 2c, 6′c, 5e), 3.95 (t, 1 H, H-4f), 3.83–3.81 (m, 4 H, OMe, H-6b), 3.64

(t, 1 H, H-5c), 3.63–3.59 (m, 2 H, H-3e, 6e), 3.53 (t, 1 H, H-6'e), 3.50–3.49 (m, 2 H, H-6f, 6'f), 3.47 (t, 1 H, H-3f), 3.44 (t, 1 H, H-4e), 3.39 (t, 1 H, H-2f), 3.36 (t, 1 H, H-2e), 3.14 (m, 1 H, H-5f), 2.22 (dd, 1 H, J_{gem}=13.7 Hz, $J_{3eq,4}$=4.8 Hz, H-3b$_{eq}$), 1.93 (t, 1 H, H-3b$_{ax}$), 2.19–1.75 (9 s, 27 H, 9 Ac); ^{13}C-NMR (100 MHz, $CDCl_3$) δ 170.7, 170.4, 170.3, 170.2, 169.7, 169.6, 168.0, 165.8, 164.1, 138.8, 138.6, 138.5, 138.4, 138.3, 137.9, 137.5, 133.2, 133.1, 129.9, 129.4, 128.4, 128.3, 128.3, 128.2, 128.2, 128.2, 128.1, 128.1, 128.0, 127.8, 127.8, 127.6, 127.5, 127.5, 127.3, 127.0, 103.7, 102.6, 101.1, 100.0, 98.6, 84.6, 82.6, 82.2, 81.6, 78.2, 77.1, 76.2, 76.2, 75.6, 75.1, 74.8, 74.7, 74.3, 73.9, 73.1, 72.0, 72.0, 71.2, 71.1, 70.3, 70.0, 68.9, 68.3, 68.2, 67.2, 67.1, 66.3, 63.3, 62.1, 61.4, 53.1, 51.5, 49.1, 35.8, 29.6, 23.2, 23.1, 21.0, 20.8, 20.7, 20.7, 20.5, 20.4, 20.3; MALDI MS: *m/z*: calcd for $C_{115}H_{128}N_2O_{38}Na$: 2,167.80; found: 2,167.91 $[M + Na]^+$.

Benzyl 2,3,4,6-tetra-O-acetyl-β-D-galactopyranosyl-(1→3)-2-acetamido-4,6-di-O-acetyl-2-deoxy-β-D-galactopyranosyl-(1→4)-{methyl 5-acetamido-4,7,8,9-tetra-O-acetyl-3,5-dideoxy-D-glycero-α-D-galacto-2-nonulopyranosylonate-(2→3)}-2,6-di-O-benzoyl-β-D-galactopyranosyl-(1→4)-2,3,6-tri-O-benzyl-β-D-glucopyranosyl-(1→6)-2,3,4-tri-O-benzyl-β-D-glucopyranoside (**24**) To a solution of compound **15** (105 mg, 64.5 μmol) and **21** (137 mg, 129 μmol) in CH_2Cl_2 (1.9 ml) was added molecular sieves 4 Å (300 mg). The suspension was stirred for 30 min and cooled to 0°C. To the mixture was added TMSOTf (1.2 μl, 6.5 μmol) and stirring was continued for 45 min. Completion of the reaction was confirmed by TLC (toluene/EtOAc=7:1). The reaction mixture was filtered through Celite. The combined filtrate and washings was extracted with $CHCl_3$, and the organic layer was washed with sat. Na_2CO_3 and brine, dried over Na_2SO_4 and concentrated. The residue was purified with column chromatography on silica gel ($CHCl_3$/MeOH=200:3) to give **24** (110 mg, 69%).; $[\alpha]_D$=+ 0.0° (*c* 0.8, $CHCl_3$); ^{1}H-NMR (600 MHz, $CDCl_3$): δ 8.18–7.09 (m, 45 H, 9 Ph), 5.88 (d, 1 H, $J_{5,NH}$=6.3 Hz, NH-c), 5.66 (m, 1 H, H-8b), 5.38–5.31 (m, 3 H, H-2a, 4c, 4d), 5.19 (dd, 1 H, $J_{6,7}$=2.3 Hz, $J_{7,8}$=9.7 Hz, H-7b), 5.15 (d, 1 H, $J_{1,2}$=8.0 Hz, H-1c), 5.11–5.07 (m, 2 H, H-3a, 2d), 5.01–4.58 (m, 17 H, H-6a, 4b, 3c, 1d, 3d, 1f, NH-b, 10 CH*H*Ph), 4.48–4.37 (m, 5 H, $J_{1,2}$=7.4 Hz, H-1a, $J_{1,2}$=8.1 Hz, H-1e, 6e, 2 CH*H*Ph), 4.29–4.22 (m, 3 H, H-9b, 2 CH*H*Ph), 4.12–3.25 (m, 28 H, H-4a, 5a, 6a, 6'a, 5b, 6b, 9'b, 2c, 5c, 6c, 6'c, 5d, 6d, 6'd, 2e, 3e, 4e, 5e, 6'e, 2f, 3f, 4f, 5f, 6f, 6'f, -OMe), 2.73 (dd, 1 H, J_{gem}=12.6 Hz, $J_{3eq,4}$=4.3 Hz, H-3b$_{eq}$), 2.19–1.49 (m, 37 H, H-3b$_{ax}$, 12 Ac); ^{13}C-NMR (150 MHz, $CDCl_3$) δ 172.1, 170.9, 170.7, 170.5, 170.3, 170.2, 170.2, 170.0, 169.3, 168.4, 165.5, 165.1, 138.9, 138.6, 138.6, 138.5, 138.1, 137.6, 133.4, 133.1, 130.3, 130.1, 130.0, 129.6, 128.7, 128.4, 128.2, 128.0, 128.0, 127.9, 127.8, 127.7, 127.7, 127.6, 127.3, 127.3, 103.8, 102.7, 101.1, 100.7, 99.0, 97.9, 84.7, 83.2, 82.4, 81.8, 78.3, 75.7, 75.2, 75.0, 75.0, 74.8, 74.5, 73.9, 73.6, 72.9, 72.2, 71.9, 71.6, 71.3, 71.0, 70.6, 69.2, 69.1, 69.0, 68.6, 67.1, 66.9, 66.6, 63.2, 62.8, 62.6, 61.0, 55.3, 52.8, 49.3, 36.9, 29.8, 24.0, 23.2, 22.8, 21.4, 20.9, 20.8, 20.8, 20.8, 20.7, 20.7, 20.4, 20.3, MALDI MS: *m/z*: calcd for $C_{127}H_{144}N_2O_{46}Na$: 2,455.89; found: 2,455.52 $[M + Na]^+$.

β-D-Galactopyranosyl-(1→3)-2-acetamido-2-deoxy-β-D-galactopyranosyl-(1→4)-{5-acetamido-3,5-dideoxy-D-glycero-α-D-galacto-2-nonulopyranosylonic acid-(2→3)}-β-D-galactopyranosyl-(1→4)-β-D-glucopyranosyl-(1→6)-β-D-glucopyranose (**1**) To a solution of compound **24** (95 mg, 39 μmol) in MeOH (1.6 ml) was added sodium methoxide (28% in MeOH; 14 mg). The mixture was stirred for 74 h under reflux condition, as the proceeding of the reaction was monitored by TLC ($CHCl_3$/MeOH/H_2O=3:2:0.3). H_2O (1.6 ml) was then added and stirring was continued for 14 h at ambient temperature. The reaction mixture was neutralized with Dowex (H^+) and filtered through cotton. The combined filtrate and washings was concentrated under diminished pressure to give a syrup compound. To a solution of the residue in H_2O (1.4 ml) was added palladium hydroxide [$Pd(OH)_2$] (20 wt% Pd on carbon; 345 mg). The mixture was vigorously stirred for 4 h at 40°C under hydrogen atmosphere, as the proceeding of the reaction was monitored by TLC (1-BuOH/MeOH/H_2O=2:1:1). The reaction mixture was filtered through Celite, and the combined filtrate and washings was concentrated. The residue was purified with gel filtration column chromatography (Sephadex LH-20, H_2O as eluent) to give **1** (43 mg, 99%).; $[\alpha]_D$=+ 0.1° (*c* 1.0, H_2O); ^{1}H-NMR (600 MHz, CD_3OD): δ 5.16 (d, 1 H, $J_{1,2}$=3.7 Hz, H-1e), 4.79 (d, 1 H, H-1c), 4.57 (d, 1 H, $J_{1,2}$=8.0 Hz, H-1d), 4.49–4.45 (m, 3 H,H-1a, 1b, 1f), 4.15–3.19 (m, 39 H, ring H), 2.62 (dd, 1 H, H-3b$_{eq}$), 1.99 and 1.96 (2 s, 6 H, 2 Ac), 1.87 (m, 1 H, H-3b$_{ax}$), ^{13}C-NMR (150 MHz, CD_3OD) δ 175.0, 174.8, 174.1, 106.1, 105.7, 105.5, 104.1, 104.0, 103.4, 101.8, 97.0, 95.3, 94.2, 93.0, 91.5, 84.4, 81.2, 78.1, 77.6, 76.5, 75.1, 74.8, 74.5, 74.3, 73.9, 73.5, 73.4, 72.6, 72.1, 71.5, 70.8, 70.2, 68.9, 68.0, 67.1, 61.2, 61.0, 60.7, 59.7, 59.3, 58.8, 52.5, 51.6, 48.8, 47.5, 28.7, 25.9, 23.5; MALDI MS: *m/z*: calcd for $C_{43}H_{72}N_2O_{34}$: 1160.40; found: 1159.75 $[M-H]^-$.

2-Acetamido-2-deoxy-β-D-galactopyranosyl-(1→4)-{5-acetamido-3,5-dideoxy-D-glycero-α-D-galacto-2-nonulopyranosylonic acid-(2→3)}-β-D-galactopyranosyl-(1→4)-β-D-glucopyranosyl-(1→6)-D-glucopyranose (**2**) To a solution of compound **23** (38 mg, 18 μmol) in MeOH (2.0 ml) was added catalytic amounts of sodium methoxide (10 mg). The mixture was stirred for 96 h under reflux conditions, as

the proceeding of the reaction was monitored by TLC (1-BuOH/MeOH/H_2O=4:1:1). H_2O was then added and stirring was continued for 10 h at ambient temperature. The reaction mixture was neutralized with Dowex (H^+) and filtered through cotton. The combined filtrate and washings was concentrated under diminished pressure to give a syrupy compound. The residue was purified by gel filtration column chromatography on Sephadex LH-20 (MeOH) to give a white solid. To a solution of the solid in MeOH/H_2O (2.5/1 ml) was added palladium hydroxide [$Pd(OH)_2$] (20 wt% Pd on carbon; 40 mg). The mixture was vigorously stirred overnight at 40°C under hydrogen atmosphere, as the proceeding of the reaction was monitored by TLC (1-BuOH/MeOH/H_2O=2:1:1). The reaction mixture was filtered through Celite. The combined filtrate and washings was concentrated. The residue was purified with gel filtration column chromatography (Sephadex LH-20, MeOH/H_2O=1:1 as eluent) using MeOH as eluent, to give **2** (18 mg, 98%).; $[\alpha]_D$=+19.4° (*c* 1.7, MeOH:H_2O=1:1); ^{1}H-NMR (500 MHz, CD_3OD/D_2O=1:1): δ 2.69 (dd, 1 H, J_{gem}=11.4 Hz, $J_{3eq,4}$=4.6 Hz, H-3b$_{eq}$), 2.04 and 2.02 (2 s, 6 H, 2 NAc), 1.91 (t, 1 H, H-3b$_{ax}$); ^{13}C-NMR (125 MHz, CD_3OD/D_2O=1:1) δ 176.0, 175.4, 175.0, 103.9, 103.9, 103.7, 102.9, 97.3, 93.4, 80.0, 78.5, 77.0, 76.1, 75.8, 75.6, 75.4, 75.1, 71.0, 70.8, 69.8, 69.6, 69.5, 69.1, 64.2, 62.3, 61.5, 61.2, 53.5, 53.0, 49.5, 49.4, 48.4, 38.0, 23.6, 22.8; MALDI MS: *m/z*: calcd for $C_{37}H_{61}N_2O_{29}$: 997.33; found: 997.25 [*M*-H]$^-$.

{5-Acetamido-3,5-dideoxy-D-glycero-α-D-galacto-2-nonulopyranosylonic acid-(2→3)}-β-D-galactopyranosyl-(1→4)-β-D-glucopyranosyl-(1→6)-D-glucopyranose (**3**) To a solution of compound **22** (45 mg, 24 μmol) in MeOH (3.0 ml) was added sodium methoxide (28% in MeOH; 11 mg). The mixture was stirred for 48 h at 45°C, as the proceeding of the reaction was monitored by TLC ($CHCl_3$/MeOH=5:1). H_2O (1.0 ml) was then added and stirring was continued for 18 h at 45°C. The reaction mixture was neutralized with Dowex (H^+) and filtered through cotton. The combined filtrate and washings was concentrated under diminished pressure to give a syrupy compound. To a solution of the residue in H_2O (2.0 ml) was added palladium hydroxide [$Pd(OH)_2$] (20 wt% Pd on carbon; 100 mg). The mixture was stirred for 8 h at ambient temperature under hydrogen atmosphere, as the proceeding of the reaction was monitored by TLC ($CHCl_3$/MeOH/H_2O=3:1:0.1). The reaction mixture was filtered through Celite. The combined filtrate and washings was concentrated. The residue was purified with gel filtration column chromatography (Sephadex LH-20, H_2O as eluent) to give **3** (14 mg, 76%).; $[\alpha]_D$=+ 8.3° (*c* 0.6, H_2O); ^{1}H-NMR (400 MHz, D_2O): δ 5.21 (d, 1 H, $J_{1,2}$=3.7 Hz, H-1e), 4.64–4.51 (m, 2 H, H-1a, 1f), 4.21–2.87 (m, 25 H, ring H), 2.75 (dd, 1 H, J_{gem}=12.0 Hz, $J_{3eq,4}$=4.6 Hz, H-3b$_{eq}$), 2.02 (s, 3 H, Ac), 1.77 (m, 1 H, H-3b$_{ax}$), ^{13}C-NMR (100 MHz, D_2O) δ 177.7, 176.6, 105.4, 105.2, 102.5, 98.7, 94.8, 80.9, 78.4, 77.9, 77.6, 77.5, 77.5, 77.0, 76.7, 75.6, 75.5, 75.4, 74.5, 74.1, 73.1, 72.2, 72.1, 71.5, 71.4, 71.1, 70.8, 70.2, 65.3, 65.2, 63.7, 62.7, 57.1, 54.4, 42.4, 24.8, 21.8, 17.7; MALDI MS: *m/z*: calcd for $C_{29}H_{24}NO_{24}$: 795.26; found: 794.24 [*M*-H]$^-$.

Acknowledgements This work was financially supported by the Ministry of Education, Culture, Sports, Science, and Technology (MEXT) of Japan (Grant-in-Aid for Scientific Research to M. K., No. 17101007), the Ministry of Health, Labour and Welfare of Japan (Health and Labour Sciences Research Grants), and CREST of JST (Japan Science and Technology Agency).

References

1. Allende, M.L., Proia, R.L.: Lubricating cell signaling pathways with gangliosides. Curr. Opin. Struct. Biol. **12**, 587–592 (2002)
2. Crocker, P.R., Paulson, J.C., Varki, A.: Siglecs and their roles in the immune system. Nat. Rev. Immunol. **7**, 255–266 (2007)
3. Holmgren, J., Lönnroth, I., Svennerholm, L.: Tissue receptor for cholera exotoxin: Postulated structure from studies with GM1 ganglioside and related glycolipids. Infect. Immunity **8**, 208–214 (1973)
4. Jolivet-Reynaud, C., Hauttecoeur, B., Alouf, J.E.: Interaction of *Clostridium perfringens* delta toxin with erythrocyte and liposome membranes and relation with the specific binding to the ganglioside GM2. Toxicon **27**, 1113–1126 (1989)
5. Fuster, M.M., Esko, J.D.: The sweet and sour of cancer: glycans as novel therapeutic targets. Nat. Rev. Cancer **5**, 526–542 (2005)
6. Jeyakumar, M., Dwek, R.A., Butters, T.D., Platt, F.M.: Storage solutions: treating lysosomal disorders of the brain. Nat. Rev. Neurosci. **6**, 1–12 (2005)
7. Feizi, T., Fazio, F., Chai, W., Wong, C.-H.: Carbohydrate microarrays: a new set of technologies at the frontiers of glycomics. Curr. Opin. Struct. Biol. **13**, 637–645 (2003) and references therein)
8. Fazio, F., Bryan, M.C., Blixt, O., Paulson, J.C., Wong, C.-H.: Synthesis of sugar arrays in microtiter plate. J. Am. Chem. Soc. **124**, 14397–14402 (2002)
9. Adams, E.W., Daniel, M.R., Bokesch, H.R., McMahon, J.B., O'Keefe, B.R., Seeberger, P.H.: Oligosaccharide and glycoprotein microarrays as tools in HIV glycobiology: Glycan–dependent gp120/protein interactions. Chem. Biol. **11**, 875–881 (2004)
10. Park, S., Shin, I.: Fabrication of carbohydrate chips for studying protein–carbohydrate interactions. Angew. Chem. Int. Ed. Engl. **41**, 3180–3182 (2002)
11. Suda, Y., Arano, A., Fukui, Y., Koshida, S., Wakao, M., Nishimura, T., Kusumoto, S., Sobel, M.: Immobilization and clustering of structurally defined oligosaccharides for sugar chips: An improved method for surface plasmon resonance analysis of protein–carbohydrate interactions. Bioconjugate Chem. **17**, 1125–1135 (2006)
12. Wang, D., Liu, S., Trummer, B.J., Deng, C., Wang, A.: Carbohydrate microarrays for the recognition of cross-reactive molecular markers of microbes and host cells. Nat. Biotechnol. **20**, 275–281 (2002)

13. Willats, W.G., Rasmussen, S.E., Kristensen, T., Mikkelsen, J.D., Knox, J.P.: Sugar-coated microarrays: A novel slide surface for the high-throughput analysis of glycans. Proteomics **2**,1666–1671 (2002)
14. Fuse, T., Ando, H., Imamura, A., Sawada, N., Ishida, H., Kiso, M., Ando, T., Li, S.-C., Li, Y.-T.: Synthesis and enzymatic susceptibility of a series of novel GM2 analogs. Glycoconjugate J. **23**, 329–343 (2006)
15. Ando, H., Koike, Y., Ishida, H., Kiso, M.: Extending the possibility of an *N*-Troc-protected sialic acid donor toward variant sialo-glycoside synthesis. Tetrahedron Lett. **44**, 6883–6886 (2003)
16. Ando, H., Imamura, A.: Proceedings in synthetic chemistry of sialo-glycoside. Trend. Glycosci. Glycotech. **16**, 293–303 (2004)
17. Yoshikawa, T., Kato, Y., Yuki, N., Yabe, T., Ishida, H., Kiso, M.: A highly efficient construction of GM1 epitope tetrasaccharide and its conjugation with KLH. Glycoconjugate J. (2008) (in press)
18. Veeneman, G.H., van Leeuwen, S.H., van Boom, J.H.: Iodonium ion promoted reactions at the anomeric centre. II An efficient thioglycoside mediated approach toward the formation of 1,2-*trans* linked glycosides and glycosidic esters. Tetrahedron Lett. **31**, 1331–1334 (1990)
19. Cook, A.F.: Use of 2,2,2-tribromoethyl chloroformate for the protection of nucleoside hydroxyl groups. J. Org. Chem **33**, 3589–3593 (1968)
20. Burke, S.D., Danheiser, R.L. (eds). Handbook of Reagents for Organic Synthesis, Oxidizing and Reducing Agents, pp. 513–518. Wiley, Chichester (1999)
21. Matsuzaki, Y., Ito, Y., Nakahara, Y., Ogawa, T.: Synthesis of branched poly-*N*-acetyl-lactosamine type pentaantennary pentacosasaccharide: Glycan part of a glycosyl ceramide from rabbit erythrocyte membrane. Tetrahedron Lett. **34**, 1061–1064 (1993)
22. Pedretti, V., Mallet, J.-M., Sinaÿ, P.: Silylmethylene radical cyclization. A stereoselective approach to branched sugars. Carbohydr. Res. **244**, 247–257 (1993)
23. Lu, W., Navidpour, L., Taylor, S.D.: An expedient synthesis of benzyl 2,3,4-tri-*O*-benzyl-β-D-glucopyranoside and benzyl 2,3,4-tri-*O*-benzyl-β-D-mannopyranoside. Carbohydr. Res. **340**, 1213–1217 (2005)
24. Debenham, S.D., Toone, E.J.: Regioselective reduction of 4,6-*O*-benzylidenes using triethylsilane and $BF_3{\cdot}Et_2O$. Tetrahedron: Asymmetry **11**, 385–387 (2000)

JOURNAL OF VIROLOGY, Apr. 2008, p. 3843–3852 Vol. 82, No. 8
0022-538X/08/$08.00+0 doi:10.1128/JVI.02013-07

Highly Enhanced Expression of CD70 on Human T-Lymphotropic Virus Type 1-Carrying T-Cell Lines and Adult T-Cell Leukemia Cells[▽]

Masanori Baba,[1]†* Mika Okamoto,[1]† Takayuki Hamasaki,[1] Sawako Horai,[2] Xin Wang,[1]‡ Yuji Ito,[3] Yasuo Suda,[4] and Naomichi Arima[2]

Division of Antiviral Chemotherapy, Center for Chronic Viral Diseases, Graduate School of Medical and Dental Sciences, Kagoshima University, Kagoshima 890-8544, Japan[1]; Division of Host Response, Center for Chronic Viral Diseases, Graduate School of Medical and Dental Sciences, Kagoshima University, Kagoshima 890-8544, Japan[2]; Department of Bioengineering, Faculty of Engineering, Kagoshima University, Kagoshima 890-0065, Japan[3]; and Nanostructured and Advanced Materials Course, Graduate School of Science and Engineering, Kagoshima University, Kagoshima 890-0065, Japan[4]

Received 11 September 2007/Accepted 30 January 2008

Human T-lymphotropic virus type 1 (HTLV-1) is the etiologic agent of adult T-cell leukemia (ATL). In Japan, the number of HTLV-1 carriers is estimated to be 1.2 million and more than 700 cases of ATL have been diagnosed every year. Considering the poor prognosis and lack of curative therapy of ATL, it seems mandatory to establish an effective strategy for the treatment of ATL. In this study, we attempted to identify the cell surface molecules that will become suitable targets of antibodies for anti-ATL therapy. The expression levels of approximately 40,000 host genes of three human T-cell lines carrying HTLV-1 genomes were analyzed by oligonucleotide microarray and compared with the expression levels of the genes in an HTLV-1-negative T-cell line. The HTLV-1-carrying T-cell lines used for experiments had totally different expression patterns of viral genome. Among the genes evaluated, the expression levels of 108 genes were found to be enhanced more than 10-fold in all of the T-cell lines examined and 11 of the 108 genes were considered to generate the proteins expressed on the cell surface. In particular, the CD70 gene was upregulated more than 1,000-fold and the enhanced expression of the CD70 molecule was confirmed by laser flow cytometry for various HTLV-1-carrying T-cell lines and primary CD4$^+$ T cells isolated from acute-type ATL patients. Such expression was not observed for primary CD4$^+$ T cells isolated from healthy donors. Since CD70 expression is strictly restricted in normal tissues, such as highly activated T and B cells, CD70 appears to be a potential target for effective antibody therapy against ATL.

Human T-lymphotropic virus type 1 (HTLV-1) is the etiologic agent of adult T-cell leukemia (ATL) and HTLV-1-associated myelopathy/tropical spastic paraparesis (10, 29, 40). The geographic distribution of the virus has been well defined, and the areas in the world where it is highly prevalent include Japan, Africa, the Caribbean islands, and South America (31). In Japan, the number of HTLV-1 carriers is estimated to be 1.2 million and more than 700 cases of ATL are diagnosed every year (37). Since conventional anticancer chemotherapy active against other lymphoid malignancies proved to be ineffective for treating aggressive types of ATL, combination chemotherapy designed exclusively for ATL has been examined. Although such chemotherapy considerably improved the treatment response rates in ATL patients, it could not sufficiently extend the median survival time (16, 39). Therefore, it seems still mandatory to establish an effective strategy for the treatment of ATL.

Monoclonal antibodies (MAbs) have recently gained considerable importance in the area of anticancer therapy. The first agent approved for clinical use is rituximab, which is an anti-CD20 mouse/human chimeric MAb (32). Rituximab was found to be effective for a variety of B-cell lymphomas as well as non-Hodgkin's lymphoma (12). Currently, several MAbs have been approved by the U.S. Food and Drug Administration for the treatment of lymphoma, leukemia, breast cancer, and metastatic colon cancer. One of the anticancer mechanisms of these MAbs is the induction of antibody-dependent cytotoxicity (15, 20). The antibodies bind to the surface antigens of tumor cells, while their crystallizable fragments (Fc) bind to the Fc receptors of the effector cells, such as natural killer cells and monocytes, triggering cytolysis of the target cells. In addition, complement-dependent cytotoxicity and direct induction of apoptosis are also considered anticancer mechanisms of the MAbs (20, 21).

A rationale of using MAbs for anticancer therapy is their high specificities to tumor cells. A certain number of antigens overexpressed on tumor cells have been identified as the targets of MAbs. Such antigens do not need to be completely absent from normal tissues, because their relative overexpression on tumor cells has proved to be sufficient to confer a high

* Corresponding author. Mailing address: Division of Antiviral Chemotherapy, Center for Chronic Viral Diseases, Graduate School of Medical and Dental Sciences, Kagoshima University, 8-35-1, Sakuragaoka, Kagoshima 890-8544, Japan. Phone: 81-99-275-5930. Fax: 81-99-275-5932. E-mail: m-baba@vanilla.ocn.ne.jp.

† These authors contributed equally to this work.

‡ Present address: Department of Pharmacology, Yale University School of Medicine, New Haven, CT 06520.

▽ Published ahead of print on 6 February 2008.

level of specificity of MAbs to the target cells (20). Nevertheless, MAbs with higher specificities would be preferable in terms of safety in vivo. Oligonucleotide microarray is an efficient tool for studying the comprehensive gene expression levels of tumor cells in comparison with normal tissues. In fact, several molecules overexpressed in ATL cells have been identified by this technology (7, 35). In these studies, clinical samples obtained from ATL patients were analyzed for their gene expression and compared with normal T cells. The advantage of this procedure is that the gene expression profiles of ATL cells in different disease types or stages can be analyzed directly. On the other hand, the expression profiles may be affected by several conditions of patients, such as the time of sample collection, the use of anticancer agents and/or other drugs, and the presence of complications. Therefore, the microarray analysis of primary ATL cells is not always an ideal way to identify the molecules commonly overexpressed in ATL cells.

The purpose of this study is to identify the surface molecules that will become potential targets for anti-ATL MAb therapy. To this end, the expression levels of approximately 40,000 host genes of three T-cell lines carrying HTLV-1 were analyzed by oligonucleotide microarray and compared with the levels in an HTLV-1-negative T-cell line. Among the genes that could be evaluated, the expressions of 108 genes were found to be enhanced more than 10-fold in all of the T-cell lines examined and 11 of the 108 genes were considered to generate the proteins expressed on the cell surface. In particular, the CD70 gene was upregulated tremendously (more than 1,000-fold), which was confirmed by the analysis for CD70 expression on various HTLV-1-carrying T-cell lines and primary $CD4^+$ T cells from ATL patients.

MATERIALS AND METHODS

Cells. The HTLV-1-carrying T-cell line S1T was established from the peripheral blood mononuclear cells (PBMCs) of an ATL patient, as described previously (2). The HTLV-1-carrying T-cell lines MT-2, MT-4, and M8166; the HTLV-1-negative T-cell lines MOLT-4, CEM, and Jurkat; and the monocytic cell lines HL-60 and U937 were also used for experiments. MT-2 and MT-4 cells are derived from umbilical cord blood lymphocytes after cocultivation with leukemia cells from ATL patients (24). MT-2 cells were reported to integrate at least eight copies, including defective types, of HTLV-1 proviral DNA in the chromosomes (18). M8166 is a subclone of C8166 cells, which were also established by cocultivation of umbilical cord blood lymphocytes with ATL cells. M8166 cells integrate one copy of provirus in the chromosome (34). All cell lines were maintained in RPMI 1640 medium supplemented with 10% heat-inactivated fetal bovine serum, 100 U/ml penicillin G, and 100 μg/ml streptomycin. PBMCs were donated under informed consent from patients with acute-type ATL and healthy volunteers. The cells were isolated from heparinized blood with Ficoll-Paque Plus (Pharmacia, Uppsala, Sweden) to obtain PBMCs. Diagnoses of ATL were based on clinical features, hematological characterization, the presence of serum antibodies against HTLV-1, and the insertion of proviral DNA into leukemia cells.

Characterization of HTLV-1-carrying T-cell lines. The production of viral antigens from S1T, MT-2, and M8166 cells into culture supernatants was determined by enzyme-linked immunosorbent assay (ELISA). Briefly, the cells (1×10^5 cells/ml) were incubated for 3 days at 37°C. After incubation, the culture supernatants were collected and examined for their p19 antigen levels with a sandwich enzyme-linked immunosorbent assay kit (Cellular Products, Buffalo, NY). The cells were also examined for their expression of HTLV-1 *env* and *tax* genes by reverse transcription-PCR (RT-PCR). For RT-PCR, the cells were harvested after a 3-day incubation and washed three times with ice-cold phosphate-buffered saline. Total RNA was extracted from the cells with an extraction kit (RNeasy; Qiagen, Hilden, Germany). The extracted RNA was treated with DNase I and subjected to RT-PCR. The primers used for RT-PCR were RENV1 (5′-ACGCCGGTTGAGTCGCGTTCT-3′), RENV4 (5′-CACCGAAGATGAG GGGGCAGA-3′), RPX3 (5′-ATCCCGTGGAGACTCCTCAA-3′), and RPX4 (5′-AACACGTAGACTGGGTATCC-3′). Glyceraldehyde-3-phosphate dehydrogenase (GAPDH) mRNA was also amplified as an internal control by the primer pair RT-GAPDH5 (5′-CATTGACCTCAACTACATGG-3′) and RT-GAPDH3 (5′-AGTGATGGCATGGACTGTGG-3′). The samples were subjected to reverse transcription to cDNA for 30 min at 42°C and PCR amplification (95°C for 30 s, 55°C for 30 s, and 72°C for 1 min) with each primer pair. The amplified products were analyzed by the 2100 Bioanalyzer (Agilent, Santa Clara, CA).

For the detection of HTLV-1 Tax, Western blot analysis of the cells was performed as described previously (41). Briefly, the cells were incubated for 3 days and lysates were obtained by treating the cells with a low-salt extraction buffer (10 mM Tris-HCl [pH 8.0] containing 0.14 M NaCl, 3 mM $MgCl_2$, 1 mM dithiothreitol, 2 mM phenylmethylsulfonyl fluoride, and 0.5% Nonidet P-40) on ice for 20 min. The lysates were centrifuged at $12,000 \times g$ at 4°C for 10 min. After measuring protein concentrations, the lysates (100 μg of protein) were electrophoresed on a 10% polyacrylamide gel with sodium dodecyl sulfate and transferred to a polyvinylidene difluoride membrane. The transferred proteins were reacted with the anti-p40 Tax MAb Lt-4 (38) or an anti-actin polyclonal antibody (Santa Cruz Biotechnology, Santa Cruz, CA), followed by treatment with horseradish peroxidase-conjugated goat anti-mouse immunoglobulin G (IgG) (Amersham Biosciences, Buckinghamshire, United Kingdom) or horseradish peroxidase-conjugated rabbit anti-goat IgG (MP Biomedicals, Solon, OH). Antibody binding was visualized with an enhanced chemiluminescence detection system (Amersham Biosciences).

Oligonucleotide microarray. S1T, M8166, MT-2, and MOLT-4 cells (1×10^5 cells/ml) were incubated for 3 days at 37°C. After incubation, total RNA was extracted from the cells with RNeasy (Qiagen). The quality of the total RNA was examined by the 2100 Bioanalyzer (Agilent), according to the manufacturer's protocol. The microarray processing of the samples was carried out with necessary reagent kits provided by Agilent, according to the manufacturer's one-color microarray-based gene expression analysis protocol (version 5.5). Briefly, 500 ng of the total RNA was reverse transcribed to cDNA with Moloney murine leukemia virus reverse transcriptase and T7 promoter primer. The cDNA was transcribed and amplified with T7 RNA polymerase to produce the cRNA labeled with cyanine 3. The cyanine 3-labeled cRNA was purified with RNeasy (Qiagen) and examined for its concentration and labeling quality by a spectrophotometer. The cRNA was fragmented and hybridized to Agilent whole human genome oligonucleotide microarray ($4 \times 44K$ slide format). After hybridization, the microarray was washed thoroughly and scanned with a microarray scanner (Agilent). The microarray scan data were processed with Future Extraction software (version 9.5.1; Agilent), according to its manual. Cell culture and microarray experiments were conducted simultaneously for all of the T-cell lines and repeated three times.

Data analysis. The expression level of each gene was analyzed by GeneSpring GX software (version 7.3.1; Agilent). Briefly, after importing the processed data into the software, they were normalized based on the default normalizing settings for one-color experiments (GeneSpring 7.3 user's guide; Agilent). The normalized data were filtered on the basis of parameters in certain specific columns of the original data files to remove the control and other inappropriate spots. The genes of which expression levels were more than 10-fold in all of the three HTLV-1-carrying T-cell lines (S1T, M8166, and MT-2) compared with the levels of the control T-cell line (MOLT-4) were selected and evaluated for their statistical significance by t test ($P < 0.05$) with multiple testing correction.

Flow cytometric analysis. The MAbs used for experiments were phycoerythrin (PE)-conjugated anti-human CD70 mouse MAbs (BD Biosciences, San Jose, CA [for staining cell lines] and BD Pharmingen, San Diego, CA [for staining PBMCs]), PE-conjugated anti-human CD124 mouse MAb (BD Biosciences), PE-conjugated anti-human interleukin-21 receptor (IL-21R) mouse MAb (R&D Systems, Minneapolis, MN), PE-conjugated anti-human CD151 mouse MAb (BD Biosciences), peridinin chlorophyll protein (PerCP)-conjugated anti-human CD3 mouse MAb (BD Biosciences), PerCP-conjugated anti-human CD4 mouse MAb (BD Biosciences), fluorescent isothiocyanate (FITC)-conjugated anti-human CD25 mouse MAb (Beckman Coulter, Fullerton, CA), FITC-conjugated anti-human CD8 mouse MAb (Beckman Coulter), PerCP-Cy5.5-conjugated anti-human CD19 mouse MAb (BD Biosciences), FITC-conjugated anti-human CD14 mouse MAb (BD Pharmingen), and their isotype-matched control MAbs. The test cell lines and PBMCs were washed with phosphate-buffered saline containing 1% bovine serum albumin and incubated with appropriate MAbs for 30 min at 4°C. After washing, the stained cells were analyzed by FACScan (Becton Dickinson, San Jose, CA).

Anti-cell proliferation assay. S1T and MOLT-4 cells were incubated (1×10^4 cells/well) in a flat-bottomed microtiter plate with an anti-human CD70 mouse MAb (BD Biosciences) or its isotype-matched control MAb at a concentration of 1 μg/ml. After incubation at 37°C, the number of viable cells was determined every day by trypan blue exclusion. For primary ATL cells, PBMCs were obtained from three different ATL patients and the cells (1×10^5 cells/well) were cultured in a microtiter plate with an anti-human CD70 mouse MAb (BD Pharmingen) or its isotype-matched control MAb at various concentrations. After a 24-h incubation, 25 μl of 3-(4,5-dimethylthiazol-2-yl)-2,5-diphenyltetrazolium bromide (MTT) (1 mg/ml) was added and further incubated at 37°C for 4 h. After incubation, 20% sodium dodecyl sulfate solution was added to each well. The plate was incubated overnight at room temperature in a dark place, and specific absorbance was read at 570 nm by a microplate reader.

RESULTS

Viral gene and antigen expression in HTLV-1-carrying T-cell lines. To identify the molecules selectively expressed in ATL cells, comprehensive gene expression in HTLV-1-carrying T-cell lines was examined by oligonucleotide microarray and compared with the gene expression in an HTLV-1-negative T-cell line. To this end, cell lines with various viral gene expression and replication patterns should be selected. Among the HTLV-1-carrying T-cell lines available in our laboratory, three T-cell lines, S1T, MT-2, and M8166, were selected and examined for their HTLV-1 gene expression, protein synthesis, and release of viral antigens in culture supernatants. The HTLV-1-negative T-cell leukemia line MOLT-4 was selected as a control. As shown in Fig. 1A, a strong signal of *tax* mRNA could be found in MT-2 and M8166 cells, whereas a significant signal of *env* mRNA was detected in only MT-2 cells. Like MOLT-4 cells, neither *env* nor *tax* mRNA was identified in S1T cells. These observations were confirmed by Western blot analysis of these cell lines, where sufficient amounts of p68 Env-Tax fusion protein and Tax were observed in MT-2 and M8166 cells, respectively (Fig. 1B). However, neither Tax nor Env could be detected in S1T cells. Furthermore, MT-2 cells produced and released a large amount of HTLV-1 p19 antigen, which is regarded as a component of viral particles, into culture supernatants, yet p19 production was not observed in M8166 and S1T cells (Fig. 1C). These results suggest that the three HTLV-1-carrying cell lines, of which viral gene expression patterns differ completely, are suitable tools for searching the host cellular genes and proteins commonly overexpressed in ATL cells obtained from patients.

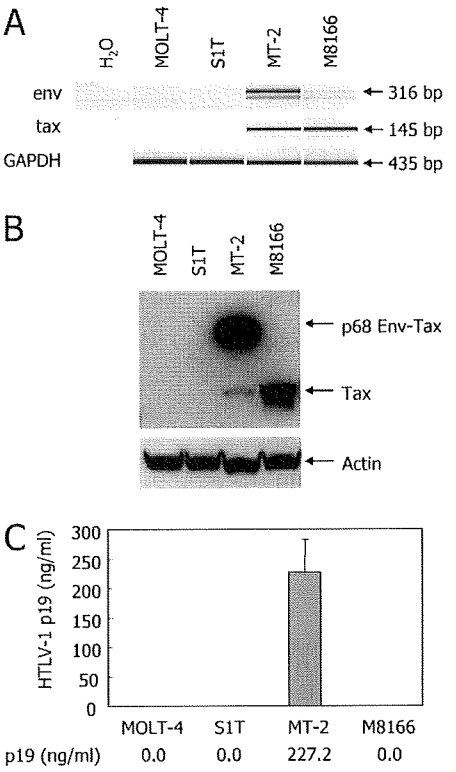

FIG. 1. Different patterns of viral gene expression in HTLV-1-carrying T-cell lines. (A) Detection of HTLV-1 *env* and *tax* gene expression in MOLT-4 (negative control), S1T, MT-2, and M1866 cells. Total RNA was extracted from the cells and subjected to RT-PCR with primer pairs described in Materials and Methods. GAPDH mRNA was also amplified as an internal control. The amplified products were analyzed by an Agilent Bioanalyzer. (B) Western blot analysis of the cells for detection of HTLV-1 Tax. The cell lysates were electrophoresed and transferred to a membrane, as described in Materials and Methods. The transferred proteins were reacted with an anti-p40 Tax MAb or an anti-actin polyclonal antibody, followed by treatment with the second antibody. Antibody binding was visualized with an enhanced chemiluminescence detection system. (C) The production of viral particles and antigens from the cells. The cells were incubated for 3 days. After incubation, culture supernatants were collected and examined for their p19 antigen levels by ELISA. The error bar indicates standard deviation.

Gene expression profiles in HTLV-1-carrying T-cell lines. The gene expression in the HTLV-1-carrying T-cell lines S1T, MT-2, and M8166 was examined and compared with the expression in the HTLV-1-negative T-cell line MOLT-4 by Agilent whole human genome oligonucleotide microarray (4×44K slide format). Among all the (41,150) genes that could be analyzed, the expression levels of 3,931 genes were modulated in all of the HTLV-1-carrying T-cell lines with statistical significance ($P < 0.05$) (data not shown). Furthermore, among the 3,931 genes, 108 genes were upregulated more than 10-fold, respectively, in all of the HTLV-1-carrying T-cell lines relative to the control cell line MOLT-4 (Table 1). When a correlation coefficient was calculated for the relative expression levels of the 108 genes in Table 1, 0.64, 0.60, and 0.96 were obtained between S1T and MT-2 cells, S1T and M8166 cells, and MT-2 and M8166 cells, respectively (data not shown). Thus, there was a positive correlation among the highly up-regulated genes of the HTLV-1-carrying T-cell lines, indicating that our strategy may be applicable for identifying the molecules commonly overexpressed in ATL cells.

From the 108 genes, 11 genes of which products were considered to be expressed on the cell surface were listed in Fig. 2. These include the genes of tumor necrosis factor (TNF) ligand superfamily member 7 (CD70), major histocompatibility complex class II (MHC II) DRβ3 (HLA-DR3B), glucose transporter member 8 (GLUT8), IL-21R (NILR), prostaglandin E receptor 4 subtype EP4 (EP4), IL-4 receptor α chain isoform a (CD124), dodecenoyl-coenzyme A δ isomerase (CD79A), CD151 antigen (GP27), TNF superfamily member 10b isoform 1 (DR5), semaphorin 4C (SEMAI), and MHC I F (HLAF). Above all, the expression of the CD70 gene was enhanced more than 1,000-fold in all of the HTLV-1-carrying T-cell lines (Table 1 and Fig. 2). Therefore, we examined whether such

TABLE 1. Genes upregulated more than 10-fold in all of the HTLV-1-carrying T-cell lines compared with the HTLV-1-negative T-cell line MOLT-4[a]

Accession no.	Symbol	Relative expression level (fold change)			Gene product
		SIT	MT-2	M8166	
NM_138410	CKLFSF7	1,886.6 ± 188.7	293.0 ± 31.0	113.3 ± 19.9	CKLF-like MARVEL transmembrane domain containing 7 isoform a
NM_001252	CD70	1,375.3 ± 137.5	2,635.3 ± 263.5	2,594.8 ± 259.5	Tumor necrosis factor ligand superfamily, member 7
NM_005572	FPL	769.8 ± 88.2	822.0 ± 155.1	1,361.6 ± 136.2	Lamin A/C isoform 2
NM_004364	CEBP	539.9 ± 191.3	87.2 ± 8.7	56.9 ± 19.8	CCAAT/enhancer binding protein α
NM_022555	HLA-DR3B	474.0 ± 93.8	14.4 ± 4.9	54.0 ± 45.3	MHC II, DRβ3 precursor
NM_004364	CEBP	468.8 ± 144.7	72.8 ± 7.3	47.1 ± 17.4	CCAAT/enhancer binding protein alpha
NM_002304	NM_002304	336.0 ± 78.3	172.3 ± 36.6	135.3 ± 16.4	
NM_002166	GIG8	331.2 ± 33.1	265.4 ± 31.0	47.3 ± 24.0	Inhibitor of DNA binding 2
NM_024644	FLJ21802	325.1 ± 32.5	108.8 ± 18.0	107.3 ± 35.1	Chromosome 14 open reading frame 169
NM_015392	CAB	275.4 ± 27.5	130.9 ± 13.1	23.4 ± 2.3	Neural proliferation 1, differentiation and control
NM_014580	GLUT8	221.3 ± 22.1	93.3 ± 13.0	116.4 ± 11.8	Solute carrier family 2, (facilitated glucose transporter) member 8
NM_024710	TMEM101	217.8 ± 37.6	228.6 ± 54.0	245.8 ± 66.3	Isochorismatase domain containing 2
NM_015691	BM042	204.4 ± 20.4	80.5 ± 8.0	34.5 ± 7.7	WWC family member 3
NM_015892	GALNAC4S-6ST	178.9 ± 18.2	40.5 ± 6.8	37.0 ± 3.8	B-cell RAG-associated protein
NM_001017535	NR1I1	140.8 ± 42.1	178.1 ± 81.8	109.3 ± 66.6	Vitamin D (1,25-dihydroxyvitamin D3) receptor
NM_033518	SN2	113.5 ± 26.6	31.5 ± 11.6	58.5 ± 22.2	Amino acid transport system N2
NM_181078	NILR	112.5 ± 11.3	127.1 ± 25.3	178.5 ± 17.8	IL-21 receptor precursor
NM_012081	ELL2	112.4 ± 23.2	52.9 ± 5.3	19.7 ± 2.0	Elongation factor 2, RNA polymerase II
	ENST00000297871	102.3 ± 10.2	82.4 ± 8.2	95.9 ± 9.6	
NM_004737	MDC1D	97.8 ± 15.4	15.8 ± 1.7	106.7 ± 26.4	Like glycosyltransferase
NM_139346	AMPH2	83.6 ± 8.4	129.0 ± 12.9	119.6 ± 12.6	Bridging integrator 1 isoform 8
NM_022121	THW	74.0 ± 7.4	29.3 ± 3.0	65.1 ± 6.6	PERP, TP53 apoptosis effector
NM_014580	GLUT8	71.7 ± 7.2	26.0 ± 3.1	31.0 ± 3.1	Solute carrier family 2, (facilitated glucose transporter) member 8
NM_004350	AML2	67.8 ± 6.8	24.9 ± 2.5	61.0 ± 6.1	Runt-related transcription factor 3 isoform 1
NM_012465	KIAA0932	65.1 ± 13.3	24.5 ± 7.7	20.2 ± 2.7	Tolloid-like 2
NM_000447	AD4	64.6 ± 9.4	87.4 ± 19.1	58.6 ± 8.1	Presenilin 2 isoform 1
NM_016010	CGI-62	63.1 ± 6.3	24.6 ± 2.5	23.5 ± 2.4	Hypothetical protein LOC51101
NM_000447	AD4	62.2 ± 12.0	90.9 ± 19.7	57.1 ± 11.1	Presenilin 2 isoform 1
NM_000786	LDM	60.9 ± 8.1	59.2 ± 11.6	63.0 ± 6.3	Cytochrome P450, family 51
NM_005658	EBI6	54.6 ± 35.4	85.3 ± 14.2	165.7 ± 71.1	TNF receptor-associated factor 1
NM_025195	C8FW	53.8 ± 19.9	170.5 ± 17.1	29.9 ± 3.7	G-protein-coupled receptor-induced protein
NM_002306	GAL3	52.1 ± 5.2	133.4 ± 14.6	81.8 ± 11.0	Galectin 3
AK057088	AK057088	51.8 ± 5.2	11.4 ± 1.1	20.4 ± 2.0	
NM_000786	LDM	50.9 ± 7.1	49.2 ± 11.5	52.6 ± 5.3	Cytochrome P450, family 51
NM_000958	EP4	50.3 ± 10.5	22.7 ± 4.6	43.0 ± 7.0	Prostaglandin E receptor 4, subtype EP4
NM_177925	MGC921	48.9 ± 4.9	134.3 ± 13.4	132.5 ± 13.3	H2A histone family, member J isoform 1
NM_003254	EPA	48.0 ± 15.7	20.1 ± 2.7	10.9 ± 3.2	Tissue inhibitor of metalloproteinase 1 precursor
NM_018094	GST2	47.4 ± 5.0	68.6 ± 6.9	68.1 ± 7.2	Peptide chain release factor 3
BC018597	TEX264	43.8 ± 4.4	51.8 ± 5.2	74.4 ± 10.0	
	THC2440229	43.7 ± 9.9	13.5 ± 4.2	11.3 ± 3.1	
NM_002200	IRF5	43.7 ± 5.3	229.9 ± 23.0	48.9 ± 7.3	Interferon regulatory factor 5 isoform a
NM_014178	amisyn	38.5 ± 3.9	200.4 ± 32.5	30.6 ± 3.1	Amisyn
NM_014417	JFY1	38.4 ± 9.4	82.8 ± 14.8	118.3 ± 49.0	BCL2 binding component 3
NM_000199	HSS	37.6 ± 4.7	10.5 ± 1.0	12.8 ± 1.4	*N*-Sulfoglucosamine sulfohydrolase (sulfamidase)
AK090416	RXRA	37.3 ± 8.1	12.3 ± 4.1	27.9 ± 10.2	FLJ00318 protein
NM_000418	CD124	37.2 ± 6.2	43.8 ± 4.4	29.6 ± 9.7	Interleukin 4 receptor α chain isoform a precursor
NM_015111	N4BP3	36.5 ± 5.5	14.2 ± 1.4	27.5 ± 2.9	Nedd4 binding protein 3
NM_015459	DKFZP564J0863	34.8 ± 6.6	26.2 ± 2.6	18.5 ± 5.4	Hypothetical protein LOC25923
NM_018664	SNFT	34.7 ± 3.5	24.6 ± 2.5	11.7 ± 2.5	Jun dimerization protein p21SNFT
NM_013385	CYT4	34.1 ± 3.4	16.2 ± 4.7	107.6 ± 34.4	Pleckstrin homology, Sec7, and coiled-coil domains 4
NR_002323	TUG1	33.4 ± 3.3	30.3 ± 3.0	30.1 ± 5.2	
BC004219	MGC4604	33.1 ± 3.3	21.0 ± 2.1	13.0 ± 3.2	1-Acylglycerol-3-phosphate *O*-acyltransferase 3
BC035647	HLA-B	33.0 ± 6.3	52.4 ± 5.2	36.3 ± 5.7	
NM_006035	MRCKB	32.0 ± 3.2	65.7 ± 6.6	74.0 ± 7.4	CDC42-binding protein kinase β
NM_001919	CD79A	31.8 ± 3.2	15.6 ± 1.7	27.2 ± 4.0	Dodecenoyl-coenzyme A δ isomerase precursor
BQ189193	ICOSLG	31.8 ± 14.2	30.1 ± 3.8	72.7 ± 7.3	
	THC2401087	31.2 ± 3.1	42.5 ± 4.2	14.6 ± 4.0	
NM_001852	MED	30.7 ± 6.6	172.2 ± 33.3	52.9 ± 5.3	α2 type IX collagen
NM_004357	GP27	30.0 ± 4.4	34.0 ± 3.4	14.5 ± 4.5	CD151 antigen

Continued on facing page